Endosomal Localization of TLR8 Confers Distinctive Proteolytic Processing on Human Myeloid Cells

Noriko Ishii,[1] Kenji Funami,[1] Megumi Tatematsu, Tsukasa Seya, and Misako Matsumoto

Nucleic acid–sensing TLRs are involved in both antimicrobial immune responses and autoimmune inflammation. TLR8 is phylogenetically and structurally related to TLR7 and TLR9, which undergo proteolytic processing in the endolysosomes to generate functional receptors. Recent structural analyses of human TLR8 ectodomain and its liganded form demonstrated that TLR8 is also cleaved, and both the N- and C-terminal halves contribute to ligand binding. However, the structures and ssRNA recognition mode of endogenous TLR8 in human primary cells are largely unknown. In this study, we show that proteolytic processing of TLR8 occurs in human monocytes and macrophages in a different manner compared with TLR7/9 cleavage. The insertion loop between leucine-rich repeats 14 and 15 in TLR8 is indispensable for the cleavage and stepwise processing that occurs in the N-terminal fragment. Both furin-like proprotein convertase and cathepsins contribute to TLR8 cleavage in the early/late endosomes. TLR8 recognizes viral ssRNA and endogenous RNA, such as microRNAs, resulting in the production of proinflammatory cytokines. Hence, localization sites of the receptors are crucial for the nucleic acid–sensing mode and downstream signaling. *The Journal of Immunology*, **2014, 193: 5118–5128.**

Discrimination between self and nonself by the innate immune system is crucial for swift elimination of infectious microbes, as well as protection against autoimmune disorders (1, 2). The compartmentalized pattern recognition receptors, including TLR3, TLR7, TLR8, and TLR9, participate in the recognition of extracellular microbial nucleic acids and transmission of innate immune signaling (3). The nucleic acid–sensing TLRs localize to the endosomal compartments (4, 5), which prevents them from responding to self nucleic acids in steady-states. The endoplasmic reticulum (ER)-resident multispan transmembrane protein UNC93B1 is indispensable for intracellular localization and signaling of these TLRs (6–10). UNC93B1 associates with TLR3, TLR7, TLR8, and TLR9 through transmembrane domains in the ER and promotes intracellular trafficking of those TLRs from the ER to the Golgi. However, the destination of each TLR is regulated by distinct determinants within TLRs (10–13).

TLR7, TLR8, and TLR9 form a subfamily of proteins that shares structural features (14, 15). Their ectodomains (ECDs) consist of 26 leucine-rich repeats (LRRs) with a large insertion loop between LRR14 and LRR15 and N- and C-terminal flanking region, LRRNT and LRRCT (16). Ligand binding to TLR–ECD induces receptor dimerization, allowing access of adaptor molecule MyD88 to the cytoplasmic Toll–IL-1R (TIR) domains (17). TLR7 and TLR8 recognize ssRNA and synthetic imidazoquinoline derivatives (18–21), whereas TLR9 recognizes CpG-containing DNA (22, 23). Accumulating evidence indicates that TLR7 and TLR9 undergo proteolytic processing in the endolysosomes of macrophages and plasmacytoid dendritic cells (pDCs) to generate functional receptors (24–29). The pH-dependent endosomal cathepsins, as well as a cysteine lysosomal protease asparaginyl endopeptidase (AEP), participate in mouse (m)/human (h)TLR9 and mTLR7 cleavage at the loop region, which is necessary for nucleic acid sensing. Hipp et al. (30) also demonstrated that hTLR7 processing is mediated with furin-like proprotein convertase. Although the truncated receptors appear to be signaling competent (26, 29), the N-terminal fragment contributes to full activation of the receptors via association with the C-terminal half (31, 32).

In humans, TLR8 is expressed in myeloid cells, including monocytes, neutrophils, macrophages, and myeloid dendritic cells (DCs), and in regulatory T cells (33–36). TLR8 recognizes viral GU-rich ssRNA and endogenous RNA, such as microRNAs within exosomes, leading to the production of proinflammatory cytokines but not type I IFNs (37, 38). Recent structural analysis of hTLR8 ECD and its ligand complex showed that TLR8 is cleaved as well, and both the N- and C-terminal halves are engaged in ligand recognition (39). However, whether the proteolytic cleavage of endogenous TLR8 actually occurs in human primary cells and how TLR8 undergoes processing remain obscure. In this study, we investigated the cleavage of TLR8 and its requirement for ligand recognition in human primary cells, including monocytes and monocyte-derived macrophages.

Materials and Methods

Cell culture, Abs, and reagents

HEK293 cells were maintained in DMEM low glucose (Invitrogen) supplemented with 10% heat-inactivated FCS (BioSource International) and antibiotics. HEK293FT cells were maintained in DMEM high glucose supplemented with 0.1 mM nonessential amino acids, 10% heat-inactivated FCS, and antibiotics. RAW264.7 cells and THP-1 cells were maintained in RPMI 1640 (Invitrogen) supplemented with 10% heat-inactivated FCS, 55 μM 2-ME (for THP-1 cells), and antibiotics. Human monocytes and B cells were isolated from PBMCs obtained from healthy individuals with a magnetic cell sorting system using anti-CD14–coated and anti-CD19–

Department of Microbiology and Immunology, Hokkaido University Graduate School of Medicine, Sapporo 060-8638, Japan

[1]N.I. and K.F. contributed equally to this work.

Received for publication May 30, 2014. Accepted for publication September 4, 2014.

This work was supported in part by grants-in-aid from the Ministry of Education, Science, and Culture, the Ministry of Health, Labor, and Welfare of Japan, and by the Akiyama Life Science Foundation.

Address correspondence and reprint requests to Dr. Misako Matsumoto, Department of Microbiology and Immunology, Hokkaido University Graduate School of Medicine, Kita 15, Nishi 7, Kita-ku, Sapporo 060-8638, Japan. E-mail address: matumoto@pop.med.hokudai.ac.jp

The online version of this article contains supplemental material.

Abbreviations used in this article: AEP, asparaginyl endopeptidase; DC, dendritic cell; ECD, ectodomain; ER, endoplasmic reticulum; h, human; LRR, leucine-rich repeat; m, mouse; MPR, mannose 6 phosphate receptor; pAb, polyclonal Ab; pDC, plasmacytoid dendritic cell; siRNA, small interfering RNA; TIR, Toll–IL-1R; TLR8-C, TLR8 C-terminal fragment; TLR8Δloop, TLR8 lacking the flexible loop between LRR14 and LRR15; TLR8-N, TLR8 N-terminal fragment.

www.jimmunol.org/cgi/doi/10.4049/jimmunol.1401375

coated MicroBeads (Miltenyi Biotec, Gladbach, Germany), respectively. Purity was checked routinely by FACS and was >95%. Monocyte-derived macrophages were differentiated from $CD14^+$ monocytes by culturing with 20 ng/ml recombinant hGM-CSF (PeproTech) for 6 d. Anti-FLAG M2 mAb, anti-FLAG polyclonal Ab (pAb), brefeldin A, z-FA-FMK, DC1 (3,3′-(5-Indolyl methylene)bis(4-hydroxycoumarin)), and LPS (*Escherichia coli* 0111:B4) were purchased from Sigma-Aldrich. In addition, the following Abs were used in this study: PE mIgG1, PE anti-human CD80 mAb, and PE anti-human CD19 mAb (all from eBioscience); FITC mIgG2b, PE anti-human CD14 mAb, and FITC anti-human CD68 mAb (all from BioLegend); Alexa Fluor– or HRP-conjugated secondary Abs (all from Invitrogen); anti-early endosome Ag 1 rabbit mAb (Cell Signaling Technology Japan); anti-GM130 mAb (BD Transduction Laboratories); anti-calnexin pAb (Stressgen; Victoria, BC, Canada); anti-p115 pAb, anti-mannose 6 phosphate receptor (MPR) pAb, anti-MPR mAb, and anti-calnexin mAb (all from Abcam, Cambridge, U.K.), anti–Lamp-1 mAb and anti–tubulin-α mAb (BioLegend); and anti-hTLR8 rabbit mAb (CST Japan). Affinity-purified rabbit pAb against hTLR8 cytoplasmic region was generated by MBL. LysoTracker Red was purchased from Invitrogen. CL075 was from InvivoGen. ssRNA40 (5′-GCCCGUCUGUUGUGUGACUC-3′, a 20-mer phosphorothioate protected ssRNA oligonucleotide) and biotinylated ssRNA40 were synthesized by Hokkaido System Science (Sapporo, Japan).

Plasmids

cDNAs for hTLR7 and hTLR8 were cloned in our laboratory by RT-PCR from the mRNA of monocyte-derived macrophages and were ligated into the cloning site of the expression vector, pEF-BOS, which was provided by Dr. S. Nagata (Kyoto University). The FLAG tag was inserted into the C terminus of pEF-BOS expression vectors for hTLR7 and hTLR8. The C-terminal FLAG-tagged TLR8 mutant lacking the flexible loop between LRR14 and LRR15 (TLR8 lacking the flexible loop between LRR14 and LRR15 [TLR8Δloop]) and the mutant lacking LRR1–14 and the flexible loop (TLR8 C-terminal fragment [TLR8-C]) were generated by PCR with KOD-Plus DNA polymerase (TOYOBO) using specific primers (forward primer: 5′-TATGGAAAAGCCTTAGATTTAAGCC-3′, reverse primer: 5′-ATAACTCTGCCGGGTATCTTTTACC-3′ for TLR8Δloop; and forward primer: 5′-TATGGAAAAGCCTTAGATTTAAGCC-3′, reverse primer: 5′-TTTGCCCACCGTTTGGGGAACTTCC-3′ for TLR8-C), as described (11). The C-terminal FLAG-tagged TLR8 mutant, R467A/R470A/R472A/R473A, was generated by site-directed mutagenesis using specific primers (forward primer: 5′-GCAGCCTCAACAGATTTTGAGTTTGACCC-3′, reverse primer: 5′-TTTCGCGATATGAGCTTGAAAAGAGGAACTATTTGC-3′). The TLR8 N-terminal fragment (LRR-NT+LRR1–14) (TLR8-N) was generated by PCR using specific primers (forward primer: 5′-CTCGAGCCACCATGAAGGAGTCATCTTTGC-3′ and reverse primer: 5′-AAAGCGGCCGCTTAATAACTCTGCCGGGTATC-3′). pEFBOS/hTLR8-FLAG-IRES-Puromycin and pEFBOS/hTLR8Δloop-FLAG-IRES-Puromycin were made in our laboratory and used for stable expression of hTLR8 and hTLR8Δloop, respectively, in RAW294.7 cells. Plasmids for human UNC93B1 (pMD2/UNC93B1) and hTLR9 (pBluescript II/TLR9) were provided by Dr. K. Miyake (The University of Tokyo) and Dr. S. Akira (Osaka University), respectively. The HA tag and FLAG tag were inserted into the C terminus of the pEF-BOS expression vector for human UNC93B1 and hTLR9, respectively.

Reporter gene assay

HEK293 cells (3×10^4 cells/well), cultured in 96-well plates, were transfected with the indicated plasmid together with the reporter plasmid and an internal control vector, phRL-TK (Promega), using FuGENE HD (Roche). The reporter plasmid containing the ELAM-1 promoter was constructed in our laboratory. Twenty-four hours after transfection, cells were stimulated with CL075 and ssRNA40 complexed to DOTAP (Roche). The cells were collected 12 h after stimulation and lysed. Firefly and *Renilla* luciferase activities were determined using a dual-luciferase reporter assay kit (Promega). The firefly luciferase activity was normalized to the *Renilla* luciferase activity and expressed as the fold induction relative to the activity in unstimulated vector-transfected cells. All assays were performed in triplicate.

RNA interference

Small interfering RNA (siRNA) duplexes (hTLR8: #s27921; negative control: #AM4635) were obtained from Ambion-Applied Biosystems. Human monocytes (5×10^5/ml) were cultured in 24-well plates with 20 ng/ml hGM-CSF. At day 4, cells were transfected with 30 pmol control or TLR8 siRNA using Lipofectamine RNAiMAX (Invitrogen). Forty-eight hours after transfection, cells were washed once and stimulated with medium or DOTAP alone, 2.5 μg/ml CL075, and ssRNA40 complexed to DOTAP for 3 h. Cells were collected by centrifugation at 1500 rpm for 3 min, and total RNA was extracted using TRIzol reagent (Invitrogen). Knockdown of hTLR8 was confirmed 48 h after siRNA transfection by quantitative PCR using specific primers (Supplemental Table I) and Western blotting with anti–TLR8-N mAb. For knockdown of TLR8 in THP-1 cells, cells were transfected with the Amaxa Cell Line Nucleofector kit V (Lonza) and 30 pmol control or TLR8 siRNA, according to the manufacturer's instructions. Nucleofection was performed twice every 24 h. Forty-eight hours postnucleofection, cells were treated with 10 ng/ml IFN-γ for 15 h and stimulated with the indicated TLR8 ligands. Experiments were repeated three times for confirmation of the results.

Quantitative PCR

Total RNA was extracted using TRIzol reagent and reverse transcribed using the high-capacity cDNA Reverse Transcription kit (Applied Biosystems) and random primers, according to the manufacturer's instructions. Quantitative PCR was performed using the indicated primers (Supplemental Table I) and the StepOne Real-Time PCR System (Applied Biosystems).

Cytokine assay

Monocyte-derived macrophages (5×10^5 /ml) were pretreated with DC1 (20 μM) or DMSO for 4 h and then were stimulated with CL075 (2.5 μg/ml), ssRNA40 complexed to DOTAP (2.5 μg/ml), or LPS (1 μg/ml) or left untreated in the presence of inhibitors for another 24 h. To examine stepwise processing of TLR8-N, monocytes were treated with 10 μM z-FA-FMK in the presence of 20 ng/ml recombinant hGM-CSF for 24 or 48 h and then stimulated with indicated ligands for 24 h. IL-12p40 in culture supernatants was measured by ELISA (R&D Systems).

Flow cytometry

Monocytes and monocyte-derived macrophages that were left untreated or stimulated with 2.5 μg/ml CL075 for 24 h were incubated with FcR Blocking Reagent, human (Miltenyi Biotec) in FACS buffer (PBS containing 5% FCS) for 5 min at 4°C and then incubated with PE mIgG1 or PE anti-human CD80 mAb (1:200) for 30 min at 4°C in the dark. For CD68 staining, cells were fixed and permeabilized by incubating with Fixation/Permeabilization Solution (BD Bioscience) for 20 min at 4°C. Cells were washed twice with 1× BD Perm/Wash buffer and incubated with FITC mIgG2b or FITC anti-human CD68 mAb (1:200) for 30 min at 4°C in the presence of mIgG2b (1:100). After washing twice with FACS buffer (for CD80 staining) or 1× BD Perm/Wash buffer (for CD68 staining), cells were analyzed on a FACSCalibur (BD Bioscience).

Immunoprecipitation

RAW264.7 cells stably expressing hTLR8-FLAG or TLR8Δloop-FLAG cultured in 10-cm dishes were lysed in 1% Nonidet P-40 lysis buffer (50 mM Tris-HCl [pH 7.5], 150 mM NaCl, 10 mM EDTA, 5 mM Na_3VO_4, 30 mM NaF, 2 mM PMSF, and a protease inhibitor mixture) for 10 min at 4°C. Lysates were clarified by centrifugation at 15,000 rpm for 15 min, precleared with protein G–Sepharose (GE Healthcare, Buckinghamshire, U.K.), and incubated with anti-FLAG mAb. The immunoprecipitates were recovered by incubation with protein G–Sepharose for 1 h at 4°C, washed three times with 1% Nonidet P-40 lysis-washing buffer (50 mM Tris-HCl [pH 7.5], 150 mM NaCl, 10 mM EDTA), and resuspended in denaturing buffer. Samples were analyzed by SDS-PAGE (7.5% gel) under reducing conditions, followed by immunoblotting with anti-FLAG pAb and anti–TLR8-N mAb.

Deglycosylation

Monocyte-derived macrophages (5.0×10^5) were lysed in 150 μl lysis buffer. After centrifugation, the supernatants were aliquoted (50 μl each) and incubated with buffer alone, 1 μl Endoglycosidase H (Roche), or 2 μl *N*-glycosidase F (Roche) for 30 min at 37°C. Samples were mixed with denaturing buffer and analyzed by SDS-PAGE under reducing conditions, followed by immunoblotting with anti–TLR8-N mAb.

Pull-down assay

Monocyte-derived macrophages (2.5×10^5 /sample) were lysed in lysis buffer, as described above. After centrifugation at 15,000 rpm for 15 min, supernatants were incubated with 2.5 μg ssRNA, biotinylated ssRNA, or 0.145 μg biotin for 1 h at 4°C. Streptavidin–Sepharose suspended in 1% BSA washing buffer was added to the reaction mixtures and incubated for 1 h at 4°C. After centrifugation, streptavidin beads were washed three times with washing buffer and resuspended in denaturing buffer for 5 min at 95°C. Samples were analyzed by SDS-PAGE under reducing conditions, followed by immunoblotting with anti–TLR8-N mAb.

Confocal microscopy

HEK293 cells (2.0×10^5 cells/well) were plated onto poly-L-lysine–coated micro coverglasses (BD Biosciences) in a 24-well plate. The following day, cells were transfected with the indicated plasmids using FuGENE HD. Twenty-four hours after transfection, cells were washed twice with PBS, fixed with 4% paraformaldehyde for 15 min, and permeabilized with PBS containing 100 μg/ml digitonin and 1% BSA. In the case of human macrophages, fixed cells (2.5×10^4 cells/well) were permeabilized with PBS containing 0.1% Triton X-100 and 2% BSA for 15 min. Fixed cells were blocked in PBS containing 1% BSA and labeled with the indicated primary Abs (2–10 μg/ml) for 60 min at room temperature. Alexa Fluor–conjugated secondary Abs (1:400) were used to visualize the staining of the primary Abs. After mounting with ProLong Gold with DAPI (Molecular Probes), cells were visualized at ×63 magnification with an LSM510 META microscope (Zeiss, Jena, Germany).

Results

Insertion loop between LRR14 and LRR15 is indispensable for hTLR8-mediated signaling

To examine the requirement of proteolytic processing in ligand recognition and signaling by hTLR8, C-terminal FLAG-tagged wild-type TLR8 and truncated mutant forms were provided. TLR8Δloop lacks the insertion loop between LRR14 and LRR15. TLR8-C represents a deletion mutant lacking LRR1–14 and the insertion loop. These were transiently expressed in HEK293 cells and stimulated with a synthetic small molecule (CL075) and ssRNA40 complexed to DOTAP. Wild-type TLR8 was expressed at the expected molecular mass (~150 kDa) and activated NF-κB in response to CL075, but not to ssRNA40, whereas TLR8Δloop failed to respond to both ligands (Fig. 1A, 1B). Cleavage products of TLR8 were undetectable in HEK293 cell lysates in either type of TLR8 expression (Fig. 1B). In addition, TLR8-C did not activate NF-κB in response to CL075 and ssRNA40 (Fig. 1A, 1B).

UNC93B1 physically associates with hTLR8 and regulates intracellular trafficking and signaling of TLR8 (10). When UNC93B1 was coexpressed with wild-type TLR8 in HEK293 cells, CL075-induced TLR8-mediated NF-κB activation was greatly increased concomitantly with the appearance of the N- and C-terminal halves of TLR8, but no response to ssRNA40 was observed (Fig. 1C, 1D). The molecular mass of the C-terminal half of TLR8 was almost the same as that of TLR8-C. In contrast, TLR8Δloop that remained uncleaved could not respond to CL075 or ssRNA40 even though it was coexpressed with UNC93B1 (Fig. 1C, 1D). Again, the

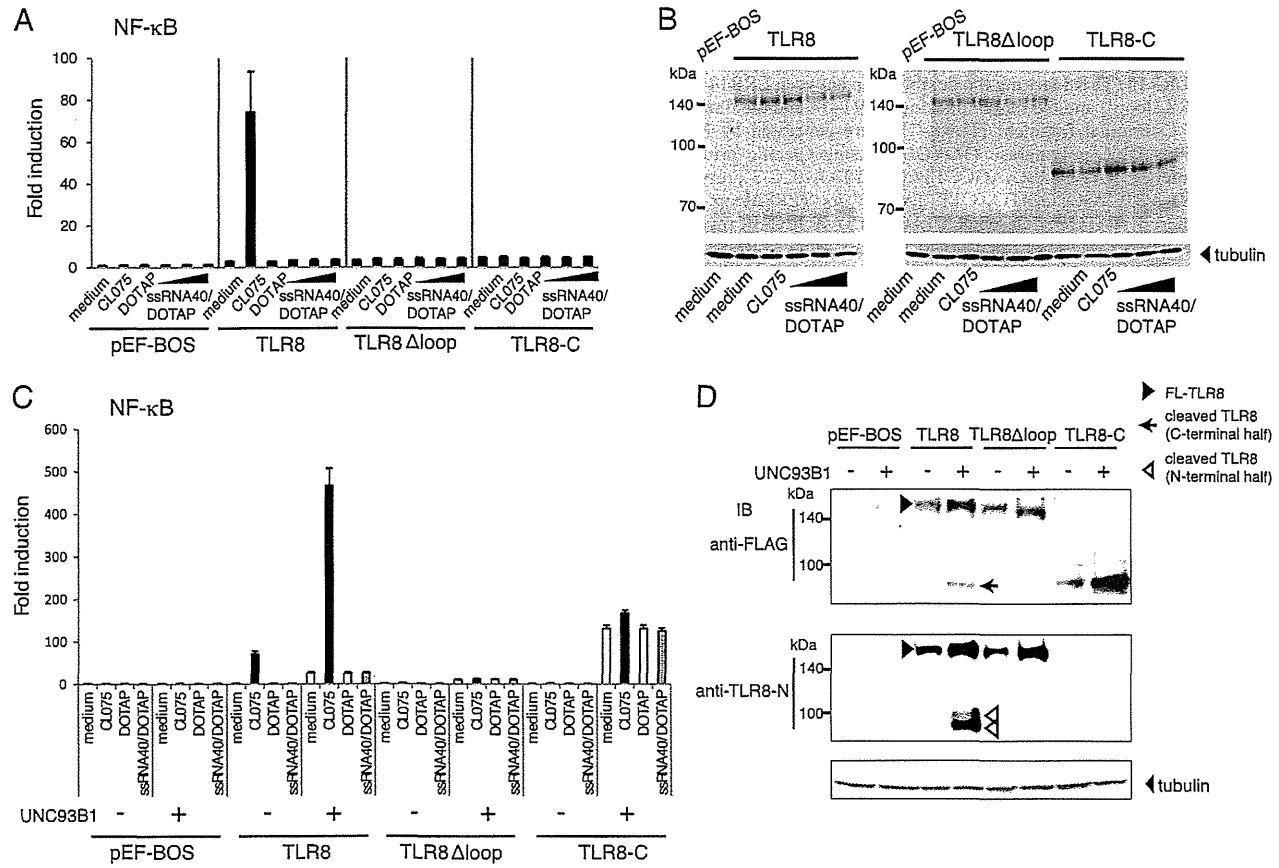

FIGURE 1. The flexible loop between LRR14 and LRR15 was required for CL075-induced TLR8-mediated NF-κB activation in HEK293 cells. (**A**) HEK293 cells were transiently transfected with vector alone or maximum amounts of C-terminal FLAG-tagged wild-type or mutant TLR8 plasmids (TLR8Δloop and TLR8-C), together with NF-κB–luciferase reporter plasmid and phRL-TK. Twenty-four hours after transfection, cells were stimulated with CL075 (2.5 μg/ml), DOTAP alone, or ssRNA40 complexed with DOTAP (2.5, 5, or 10 μg/ml) or were left untreated. Luciferase activity was measured 12 h after stimulation and expressed as fold induction relative to the activity of unstimulated cells. Representative data from three independent experiments, each performed in triplicate, are shown (mean ± SD). (**B**) Protein expression of wild-type and mutant TLR8 in HEK293 cells. Cell lysates prepared in (A) were subjected to SDS-PAGE (7.5%), followed by Western blotting with anti-FLAG mAb and anti–tubulin-α mAb. (**C**) Coexpression of UNC93B1 promoted CL075-induced TLR8-mediated NF-κB activation in HEK293 cells. HEK293 cells were transfected with the indicated plasmids together with NF-κB–luciferase reporter plasmid and phRL-TK. Cells were stimulated with 2.5 μg/ml CL075, DOTAP alone, or ssRNA40 complexed to DOTAP or were left untreated. Luciferase activity was measured 12 h after stimulation and expressed as fold induction relative to the activity of unstimulated cells. (**D**) Cell lysates prepared in (C) were subjected to SDS-PAGE (7.5%), followed by Western blotting with anti-FLAG mAb, anti–TLR8-N mAb, and anti–tubulin-α mAb. Filled arrowheads indicate full-length TLR8. Open arrowheads indicate N-terminal half of TLR8. Arrow indicates C-terminal half of TLR8.

truncated C-terminal half of TLR8 was unable to act as an RNA-sensing receptor. These results suggest that the loop region between LRR14 and LRR15 is crucial for ligand-induced TLR8-mediated signaling, as well as proteolytic processing of TLR8. UNC93B1 promoted proteolytic cleavage of TLR8 by facilitating ER exit of TLR8. In HEK293 cells transiently expressing TLR8, small amounts of cleaved TLR8 molecules appear to participate in the recognition of CL075 (Fig. 1A). Although the reason why ssRNA40 could not activate TLR8 in HEK293 cells ectopically expressing UNC93B1 is unclear, one possible interpretation is that oligomerization of multiple TLR8 molecules is required for ssRNA40-induced NF-κB activation. Notably, overexpressed wild-type and mutant TLR8, especially TLR8-C, activate NF-κB in a ligand-independent manner only when coexpressed with UNC93B1 (Fig. 1C, Supplemental Fig. 1), suggesting that transient overexpression and trafficking may allow TLR8–TIR domains to access each other, leading to activation of downstream signaling.

Cleavage of endogenous TLR8 in IFN-γ–treated THP-1 cells

THP-1 cells expressed TLR8 mRNA, which was upregulated by stimulation with IFN-γ (Fig. 2A) (40). To examine the structure of endogenous TLR8, we generated a pAb that recognizes the hTLR8 C-terminal peptides. The anti–TLR8-C pAb specifically recognized the full-length and C-terminal half of TLR8 but not N-terminal half of TLR8, hTLR7, or hTLR9 (Supplemental Fig. 2). In the IFN-γ–treated THP-1 cells, both full-length and C-terminal half of TLR8 proteins were detected by Western blotting with anti–TLR8-C Ab, indicating that endogenous TLR8 undergoes proteolytic processing (Fig. 2B). IFN-γ–treated THP-1 cells induced IL-12p40 mRNA expression in response to CL075, as well as ssRNA40, which was abolished by TLR8 knockdown (Fig. 2C).

Cleaved form of TLR8 is predominant in human primary monocytes and monocyte-derived macrophages

We investigated structural features of endogenous TLR8 in human primary cells, including monocytes and monocyte-derived macrophages. $CD14^+$ monocytes were successfully differentiated into macrophages after GM-CSF treatment for 6 d, in which the macrophage marker CD68 was greatly induced and the costimulatory molecule CD80 was upregulated by stimulation with CL075 (Supplemental Fig. 3). Immunoblotting with anti–TLR8-N and anti–TLR8-C Abs under reducing or nonreducing conditions clearly showed that TLR8 underwent proteolytic processing, and cleaved forms of TLR8 were predominant in monocytes and monocyte-derived macrophages (Fig. 3A). The TLR8 N-terminal halves consisted of two bands with a molecular mass ~100 and ~90 kDa. The C-terminal half was detected as a single band with a molecular mass ~90 kDa (Fig. 3A). None of the bands corresponding to TLR8 was observed in B cells, confirming the specificity of the TLR8 Abs used.

Upon stimulation with CL075 or ssRNA40 complexed to DOTAP, monocyte-derived macrophages produced a high level of IL-12p40 and some IL-6 and TNF-α, but their expression varied among different donors/individuals (Fig. 3B). Human monocyte-derived macrophages expressed low levels of TLR7; therefore, we examined whether the response to CL075 and ssRNA40 depended on TLR8 by knockdown analysis in macrophages. CL075- and ssRNA40-induced IL-12p40 mRNA expression was significantly reduced when TLR8 expression was knocked down at both the mRNA and protein levels (Fig. 3C). Notably, the expression and processing of TLR8 were mostly unaltered during differentiation from $CD14^+$ monocytes to macrophages, with the exception of day-1 monocytes after GM-CSF treatment: full-length TLR8 disappeared, and the lower band of TLR8-N was detected primarily (Fig. 4A). The response of TLR8 to ssRNA40 was unchanged during differentiation (Fig. 4B). Absence of full-length TLR8 at day 1 upon differentiation of monocytes with GM-CSF was observed consistently, irrelevant of the donor. These results suggest that the cleaved form of TLR8 is a functional receptor in human primary cells.

Both furin-like proprotein convertase and cathepsins are involved in stepwise processing of hTLR8

Two TLR8-Ns with different molecular masses were detected in monocyte and macrophage lysates; thus, we examined the proteases involved in TLR8 cleavage in human primary cells using protease inhibitors. Treatment of macrophages with z-FA-FMK, a cysteine protease inhibitor that blocks cathepsin proteolytic activity, failed to reduce both TLR8 cleavage and response to TLR8 agonists, probably because the cleaved form of TLR8 was abundant in macrophages (data not shown). When monocytes were differentiated into macrophages with GM-CSF in the presence of z-FA-FMK, an ~100-kDa upper band of TLR8-N accumulated from days 1 to 3, compared with DMSO-treated monocyte differentiation that mainly contained the lower band of TLR8-N (Fig. 5A, *upper panels*). This suggests that the upper band of TLR8-N is

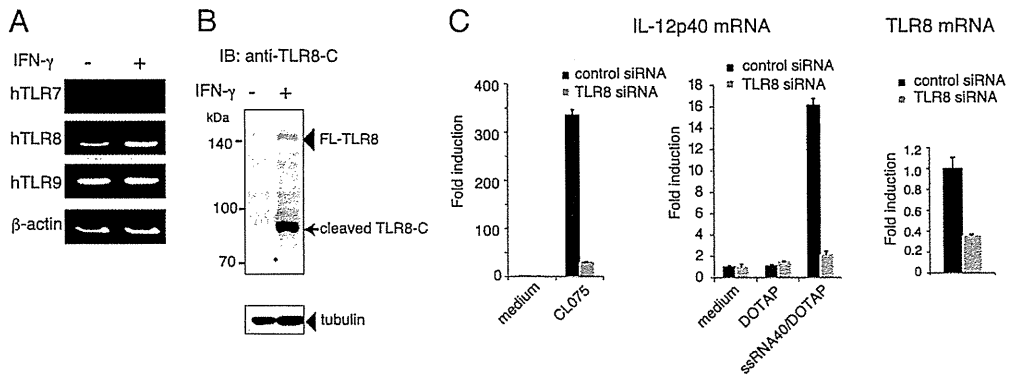

FIGURE 2. Human TLR8 underwent proteolytic processing in IFN-γ–treated THP-1 cells. **(A)** THP-1 cells (5×10^5/ml) were stimulated with 20 ng/ml IFN-γ or were left untreated for 15 h. Expression of TLR7, TLR8, and TLR9 mRNAs was analyzed by RT-PCR using specific primers (Supplemental Table I) (56). **(B)** Lysates of IFN-γ–treated or untreated THP-1 cells were subjected to SDS-PAGE, followed by Western blotting with anti–hTLR8-C pAb and anti–tubulin-α mAb. Arrowhead indicates full-length TLR8. Arrow indicates C-terminal half of TLR8. **(C)** Control or TLR8–knocked down IFN-γ–treated THP-1 cells (5×10^5/ml) were stimulated with medium alone, 2.5 μg/ml CL075, DOTAP alone, or 2.5 μg/ml ssRNA40 complexed to DOTAP. After 12 h, total RNA was extracted, and quantitative PCR was performed using primers for the IL-12p40 and TLR8 genes. Expression of genes was normalized to β-actin mRNA expression. Knockdown efficiency is shown (*right panel*). Representative data from two independent experiments are shown (mean ± SD).

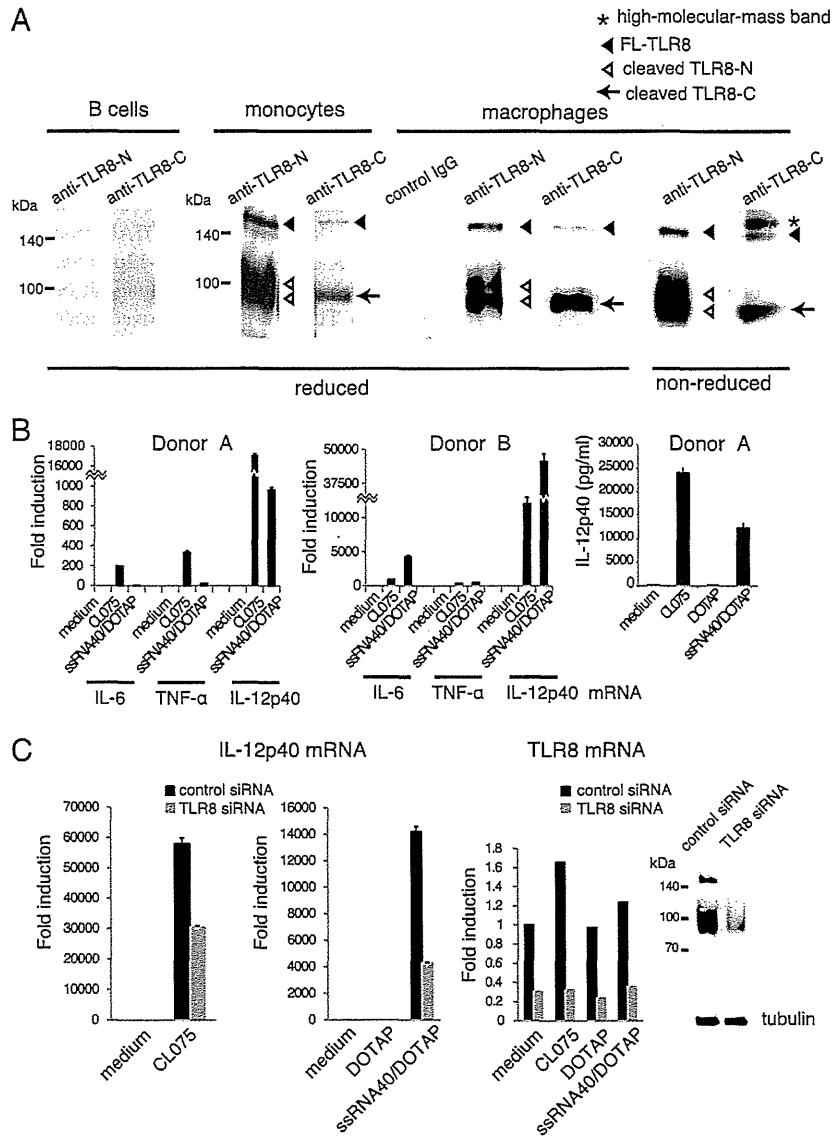

FIGURE 3. Cleaved form of TLR8 was predominant in human monocytes and monocyte-derived macrophages. (**A**) Lysates of human monocytes and monocyte-derived macrophages were subjected to SDS-PAGE under reducing or nonreducing conditions, followed by Western blotting with anti–TLR8-N mAb, anti–TLR8-C pAb, or control rabbit IgG. Lysates of B cells were used as cellular negative control. Filled arrowheads indicate full-length TLR8 (~150 kDa). Open arrowheads indicates N-terminal halves of TLR8 (~100 and ~90 kDa). Arrows indicate C-terminal half of TLR8 (90 kDa). Asterisk indicates high molecular mass band of TLR8. (**B**) Human monocyte-derived macrophages from different healthy donors were stimulated with the indicated ligands for 3 h, and IL-6, IL-12p40, and TNF-α transcripts were measured by quantitative PCR (*left* and *middle panels*). Protein levels of IL-12p40 in culture supernatants after 24 h of stimulation (donor A) were quantified using ELISA (*right panel*). (**C**) TLR8 is indispensable for ssRNA-induced cytokine production by human macrophages. Monocyte-derived macrophages (5×10^5/ml) were transfected with 30 pmol control or TLR8 siRNA. Forty-eight hours after transfection, cells were washed and stimulated with medium alone, 2.5 μg/ml CL075, DOTAP alone, or 2.5 μg/ml ssRNA40 complexed to DOTAP for 3 h, and IL-12p40 mRNA was measured by quantitative PCR. Knockdown of TLR8 mRNA and protein was confirmed by quantitative PCR and Western blotting with anti–TLR8-N mAb, respectively. Representative data from three independent experiments are shown (mean ± SD).

a premature form, and cysteine proteases, such as the cathepsin family, participate in further processing to generate the mature form of TLR8-N. Correlatively, when day-1 and day-2 monocytes were stimulated with CL075 or ssRNA40 complexed to DOTAP for 24 h, IL-12p40 production was decreased in z-FA-FMK–treated monocytes compared with DMSO-treated cells (Fig. 5A, *lower panel*). Considering that TLR7 was barely expressed in day- 1 to day-3 differentiated monocytes, involvement of TLR7 in CL075-induced IL-12p40 production is minimal, at best, under these experimental conditions. LPS-induced IL-12p40 production by these differentiated monocytes was unaltered in the presence of z-FA-FMK (data not shown).

A recent study demonstrated that furin-like proprotein convertase participates in processing of hTLR7 (30). We assessed the role of furin-like proprotein convertase in hTLR8 processing. Inhibition of furin-like proprotein convertase using DC1 reduced the response of macrophage TLR8 to CL075 and ssRNA40 but not to LPS (Fig. 5B). The cleaved TLR8-C and two TLR8-Ns, especially the upper band of TLR8-N, were reduced in DC1-treated macrophages compared with DMSO-treated cells (Fig. 5B, data not shown). Because a potential furin-like proprotein convertase–recognition site is present in the flexible loop between LRR14 and LRR15 of hTLR8, we made TLR8 mutant R467A/R470A/R472A/R473A in which the arginine residues in the potential furin-like proprotein convertase–recognition site in the flexible loop were substituted with alanine. This TLR8 mutant completely failed to undergo proteolytic processing when ectopically expressed in HEK293 cells, with or without UNC93B1, resulting in no activation of NF-κB in response to CL075 (Fig. 5C). These results indicate that furin-like proprotein convertase is indispensable for TLR8 cleavage at an initial step. Thus, both furin-like proprotein convertase and cathepsins are involved in stepwise processing of TLR8-N in human primary monocytes and macrophages.

N- and C-terminal halves of hTLR8 associate with each other and ssRNA40 binds to the cleaved/associated TLR8

To explore the association of the N- and C- terminal halves of TLR8, C-terminal FLAG-tagged wild-type and mutant hTLR8 were stably expressed in the mouse macrophage cell line RAW264.7. Wild-type TLR8, but not TLR8Δloop, underwent proteolytic processing in RAW cells, similar to an endogenous TLR8 in human macrophages (Fig. 6A). The N-terminal half of TLR8 coimmunoprecipitated with the C-terminal half of TLR8 under reducing and nonreducing conditions, suggesting that both the N- and

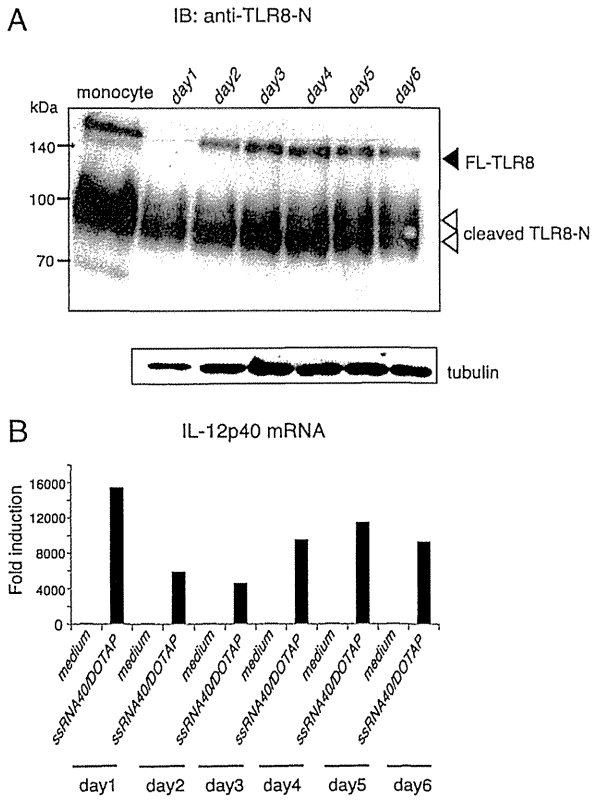

FIGURE 4. Expression and proteolytic processing of hTLR8 during differentiation from monocytes to macrophages. (**A**) $CD14^+$ human monocytes were cultured in medium containing GM-CSF for 1–6 d. TLR8 protein in differentiating cells was analyzed by western blotting with anti–TLR8-N mAb. Filled arrowhead indicates full-length TLR8. Open arrowheads indicate cleaved N-terminal halves of TLR8. (**B**) Response to ssRNA40 during differentiation from monocytes to macrophages. Differentiating cells were stimulated with 2.5 μg/ml ssRNA40 complexed to DOTAP for 3 h, and IL-12p40 transcript was measured by quantitative PCR. Representative data from more than three independent experiments are shown. In every experiment, full-length TLR8 was absent at day 1 upon differentiation of monocytes to macrophages after GM-CSF treatment.

C-terminal halves were noncovalently associated with each other in macrophages (Fig. 6B). We examined the interaction of ssRNA with TLR8 by pull-down assay using human macrophage lysates and biotinylated ssRNA40. After incubation of biotinylated ssRNA40 in the human macrophage lysates, ssRNA40–receptor complex was pulled down with avidin-Sepharose. Both the N- and C-terminal halves of TLR8 were pulled down, indicating that ssRNA40 bound to the cleaved/associated form of TLR8 (Fig. 6C).

Intracellular trafficking of hTLR8

TLR8 localizes to the ER and early endosome in primary human monocytes and HeLa cells transiently expressing hTLR8 (10). We examined the glycosylation of TLR8 protein in monocyte-derived macrophages with Endoglycosidase H, which hydrolyzes the high-mannose type *N*-glycans and *N*-glycosidase F that cleaves all types of asparagine-bound *N*-glycans. Deglycosylation analysis clearly showed that TLR8 was cleaved after passing through the Golgi, because most of the sugars on the cleaved TLR8-N were resistant to Endoglycosidase H and sensitive to *N*-glycosidase F (Fig. 7A). In contrast, N-linked sugars on full-length TLR8 were sensitive to Endoglycosidase H, indicating that an ~150-kDa band corresponding to full-length TLR8 was derived from the ER (Fig. 7A). The full-length TLR8 proteins accumulated in macrophages by brefeldin A treatment that disrupted the Golgi pathway (Fig. 7B).

Coexpression of UNC93B1 with TLR8 facilitated intracellular trafficking of TLR8 in HEK293 cells, resulting in accumulation of cleaved TLR8 (Fig. 1D). Confocal immunofluorescence analysis demonstrated that colocalization of TLR8 with p115 (Golgi-resident protein) was increased by UNC93B1 coexpression (Fig. 8A). TLR8 colocalized with MPR (late endosome marker protein), but not LysoTracker (lysosome marker), in UNC93B1-expressing cells (Fig. 8A). In human monocyte-derived macrophages, TLR8 colocalized with early endosome Ag 1 (early endosome marker protein), MPR, and calnexin (ER protein) but not with Lamp-1 (lysosome marker protein) (Fig. 8B). Taken together, these results indicated that TLR8 exits the ER, passes through the Golgi, and is targeted to early/late endosomes where the processing occurs.

Discussion

In the current study, we showed for the first time, to our knowledge, that proteolytic processing of TLR8 occurs in human primary cells, including monocytes and monocyte-derived macrophages, in a different manner from that of TLR7 and TLR9 cleavage. The insertion loop between LRR14 and LRR15 in TLR8 ECD is indispensable for cleavage and stepwise processing that occurs in the N-terminal fragment. Both furin-like proprotein convertase and cathepsins contribute to TLR8 cleavage in the early/late endosomes. Recent structural analysis of hTLR8 ECD–chemical ligand complex demonstrated that purified TLR8 ECD protein is cleaved at the loop region, and the N- and C-terminal halves remain associated, which contributes to ligand recognition and dimerization (39). Indeed, noncovalent association of the N-terminal half of TLR8 with the C-terminal half was detected by immunoprecipitation assay in RAW macrophages stably expressing hTLR8 (Fig. 6B). Furthermore, a pull-down assay revealed that ssRNA bound to the cleaved/associated form of TLR8 in human macrophages (Fig. 6C).

TLR8 belongs to the same subfamily as TLR7 and TLR9 (14, 15), but localization and signaling are quite different. We showed that hTLR8 localized to the ER and the early/late endosomes, but not to the lysosome, in monocytes and macrophages (Fig. 8B) (10), whereas mTLR7 and mTLR9 localized to the endolysosomes of macrophages and pDCs (8). The pH-dependent cathepsin family and AEP are involved in the stepwise processing of TLR7 and TLR9 at the C-terminal portion in mouse macrophages and DCs, although their contribution depends on cell type (24–29). In contrast, hTLR7 is processed at neutral pH, which is mediated with furin-like proprotein convertase (30). In the case of hTLR8, cathepsins mediate second-step processing of the N-terminal half, resulting in the generation of the mature form of the N-terminal half (Fig. 5A). Like hTLR7 processing, furin-like proprotein convertase is indispensable for TLR8 cleavage at an early step (Fig. 5B, 5C). Indeed, potential furin-like proprotein convertase–recognition sites are present in LRR14 and the flexible loop of hTLR8; one such site is located just before the N-terminus of the C-terminal ECD fragment (39). The TLR8 mutant R467A/R470A/R472A/R473A, in which arginine residues in the potential furin-like proprotein convertase–recognition site were substituted with alanine, was uncleaved when ectopically expressed in HEK293 cells and failed to transmit signals upon stimulation with CL075 (Fig. 5C). Although a putative asparagine cleavage site for AEP is found in the flexible loop of hTLR8 compared with that of mTLR7/9 (27), this site is located within the TLR8-C sequence, suggesting that AEP does not participate in TLR8 cleavage. Thus, proteases involved in processing of TLR7, TLR8, and TLR9 appear to be different and might depend on the localization of receptors and species- and cell type–specific protease distribution.

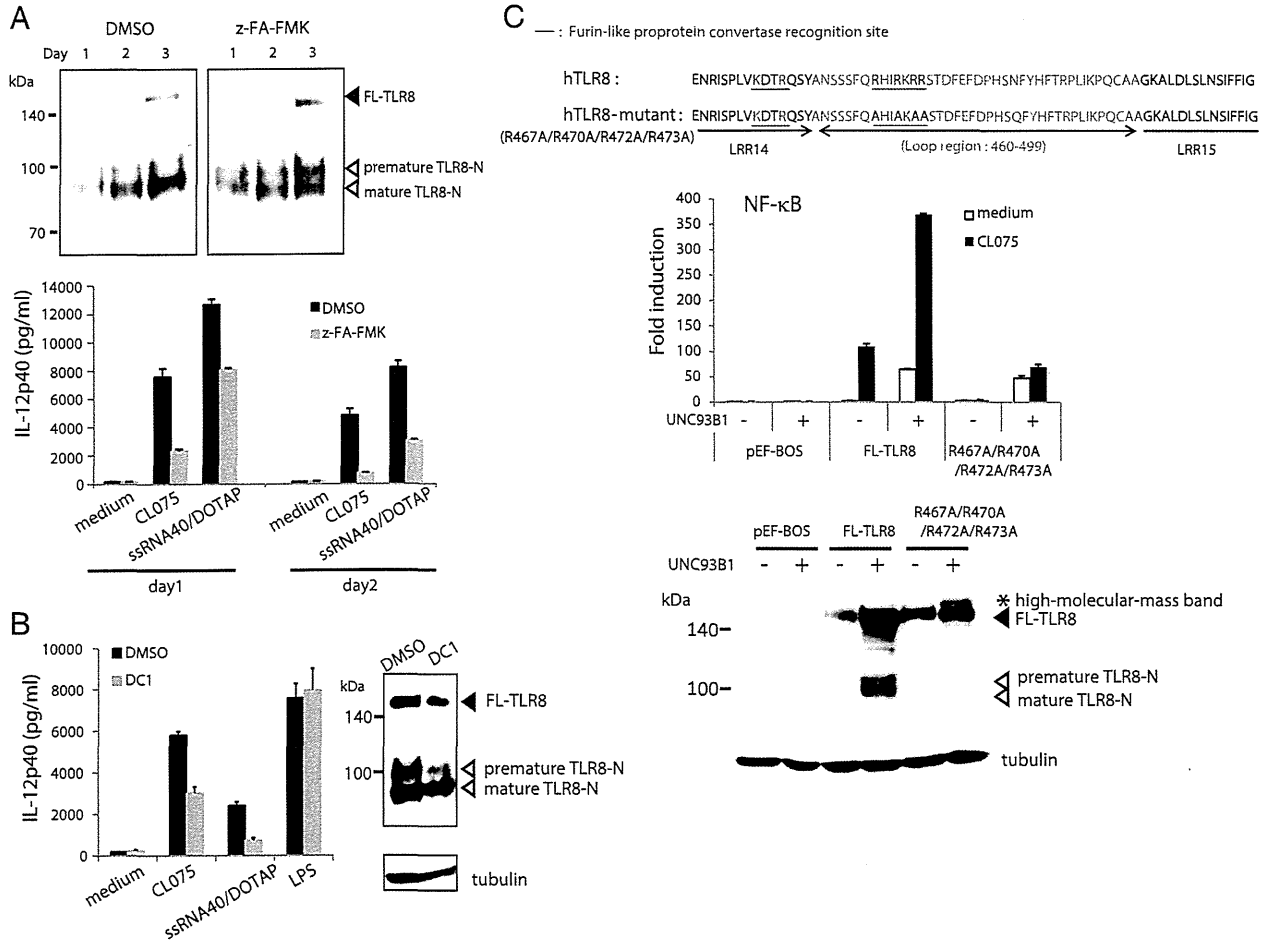

FIGURE 5. Furin-like proprotein convertases and cathepsins are involved in stepwise processing of hTLR8. (**A**) Monocytes were treated with GM-CSF in the presence or absence of 10 μM z-FA-FMK for up to 3 d. At day 1, day 2, and day 3, cells were lysed, and lysates were subjected to SDS-PAGE under reducing conditions, followed by Western blotting with anti–TLR8-N mAb (*upper panels*). The day-1 and day-2 monocytes were stimulated with medium alone, CL075 (2.5 μg/ml), or ssRNA40 complexed to DOTAP (2.5 μg/ml) for 24 h. IL-12p40 in the culture supernatants was measured using ELISA (*lower panel*). (**B**) Monocyte-derived macrophages were pretreated with 20 μM DC1 for 4 h and then stimulated with medium alone, CL075 (2.5 μg/ml), ssRNA40 complexed to DOTAP (2.5 μg/ml), or LPS (1 μg/ml) for 24 h. IL-12p40 in the culture supernatants was measured using ELISA (*left panel*). Lysates of DC1-treated macrophages were analyzed by Western blotting with anti–TLR8-N mAb and anti–tubulin-α mAb (*right panel*). (**C**) The potential furin-like proprotein convertase–recognition sites in LRR14 and insertion loop of hTLR8 (*upper panel*). Furin-like proprotein covertase–recognition site is R/K-Xn-R/K (X, any amino acid residue; n = 0, 2, 4, or 6). HEK293 cells were transfected with empty vector, wild-type TLR8 or R467A/R470A/R472A/R473A TLR8 mutant plasmid together with NF-κB–luciferase reporter plasmid and phRL-TK (*middle panel*). Cells were stimulated with 2.5 μg/ml CL075 or were left untreated. Luciferase activity was measured 12 h after stimulation and expressed as fold induction relative to the activity of unstimulated cells (mean ± SD). Cell lysates prepared in the reporter assay (medium stimulation) were subjected to SDS-PAGE (7.5%), followed by Western blotting with anti–TLR8-N mAb and anti–tubulin-α mAb (*bottom panel*). Closed arrowhead indicates full-length TLR8. Open arrowheads indicate premature and mature TLR8-N. Asterisk indicates high molecular mass band of TLR8. Representative data from two independent experiments are shown.

In freshly isolated human monocytes, cathepsins B and L are distributed in endosomes rather than lysosomes, and their sp. act. is observed in endosomal, but not in lysosomal, fractions (41). In addition, both cathepsins are expressed in HEK293 and THP-1 cells, whereas cathepsin S is expressed in THP-1 cells but not in HEK293 cells (K. Iwano, A. Watanabe, and M. Matsumoto, unpublished data). Considering the endosomal, but not lysosomal, localization of hTLR8, stepwise processing of hTLR8 by furin-like proprotein convertase and members of the cathepsin family, such as cathepsins B and L, might occur in early/late endosomes.

UNC93B1 mediates ER exit of TLR8, resulting in the accumulation of cleaved TLR8 in HEK293 cells (Fig. 1D). Notably, the TLR8-activating ability was different between CL075 and ssRNA40 in HEK293 cells transiently expressing TLR8 (Fig. 1). Structural analysis of unliganded and liganded TLR8 ECD revealed that cleaved/associated TLR8 dimerizes without ligand, and ligand binding to both N- and C-terminal halves induces structural reorganization of the TLR8 dimer (39). Mutagenesis analysis showed that interaction sites of TLR8 ECD with ssRNA appear to differ from those with chemical ligands. Oligomerization of TLR8 dimer might be required for ssRNA-induced signaling like dsRNA-induced TLR3-mediated signaling (42). In HEK293 cells, a small number of cleaved/associated TLR8 molecules is unable to induce signals to activate NF-κB in response to ssRNA40. In any case, our cellular analysis indicates that cleaved/associated TLR8 is responsible for recognition of both chemical ligands and ssRNA, and it induces innate immune responses in human primary cells.

Recent reports showed that dsRNA-sensing TLR3 undergoes cathepsin-mediated cleavage in a cell type–dependent manner (43–45). In addition, TLR3 recognizes incomplete stem structures formed in ssRNA (46). The nucleic acid–sensing TLRs respond to

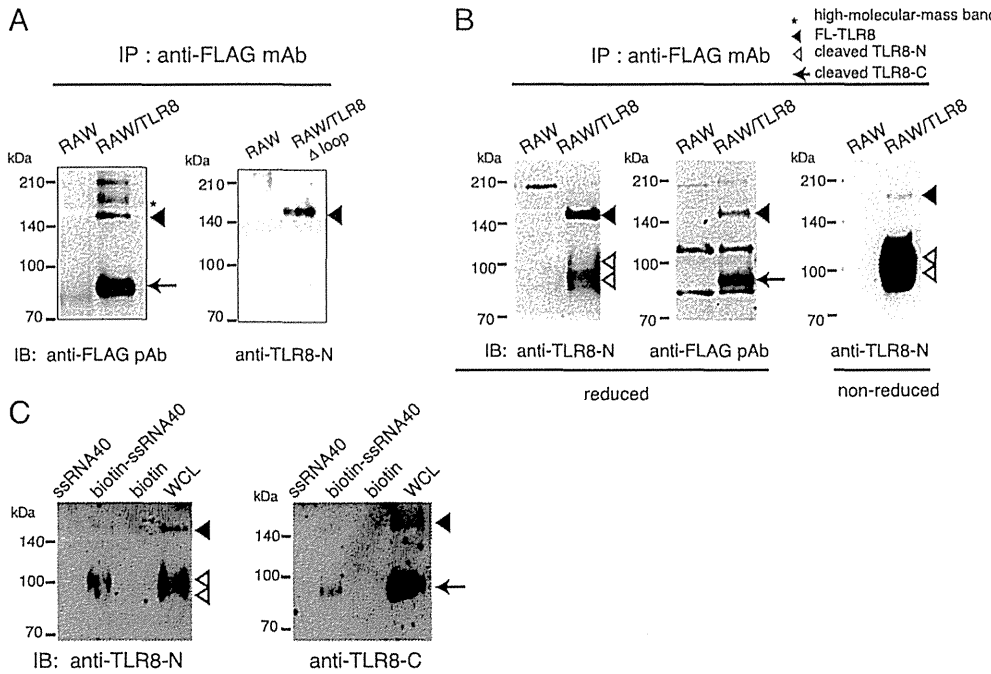

FIGURE 6. The N-terminal half of TLR8 is noncovalently associated with the C-terminal half. (**A**) Immunoblot analysis of RAW264.7 cells stably expressing C-terminal FLAG-tagged hTLR8 or hTLR8Δloop mutant. Cell lysates were immunoprecipitated (IP) with anti-FLAG mAb. The immunoprecipitates were resolved by SDS-PAGE, followed by immunoblotting (IB) with anti-FLAG pAb or anti–TLR8-N mAb. (**B**) Cell lysates of RAW264.7 cells stably expressing C-terminal FLAG-tagged hTLR8 were immunoprecipitated with anti-FLAG mAb. The immunoprecipitates were resolved by SDS-PAGE under reducing and nonreducing conditions, followed by immunoblotting with anti–TLR8-N mAb. The blot was reprobed with anti-FLAG pAb (*middle panel*). The ~210-kDa band is a nonspecific band observed in RAW cells. (**C**) ssRNA40 bound to the cleaved TLR8. Lysates of human macrophages were incubated with ssRNA40 (2.5 μg), biotinylated ssRNA40 (2.5 μg), or biotin (0.145 μg) or were left untreated for 1 h at 4°C and pulled down with streptavidin-Sepharose. Samples were analyzed by SDS-PAGE under reducing conditions, followed by immunoblotting with anti–TLR8-N mAb and anti–TLR8-C pAb.

microbial nucleic acid, as well as to endogenous self nucleic acids, in a sequence-independent, but motif-dependent, manner. Hence, the cleaved/associated form of receptors might be beneficial for recognition of nucleic acids with different nucleotide sequences and structures (47).

The role of TLR8 in antiviral immunity in humans remains unknown. In the case of HIV infection, TLR8 signaling appears to benefit HIV replication (48), but another study demonstrated an anti-HIV function for TLR8 (49). TLR8 expressed in neutrophils mediates neutrophil extracellular trap formation in HIV-1 infection via recognition of viral nucleic acids, which is useful for HIV-1 elimination (50). In addition, TLR8-mediated IL-12p70 production by monocytes polarizes naive $CD4^+$ T cells into Th1 cells that mediate cellular immunity (51). Thus, TLR8 triggers important antimicrobial signals in distinctive cells that express TLR8 but not other nucleic acid–sensing TLRs.

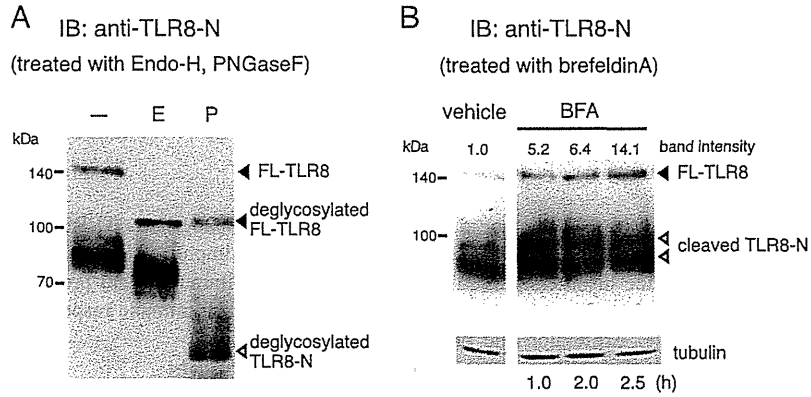

FIGURE 7. Cleaved TLR8 was generated after traveling through the Golgi. (**A**) Immunoblot (IB) analysis of monocyte-derived macrophage lysates (5×10^5) incubated with 1 μl Endoglycosidase H (E) or 2 μl *N*-glycosidase F (P) for 30 min at 37°C. Anti–TLR8-N mAb was used to detect full-length and cleaved TLR8. (**B**) Accumulation of full-length TLR8 by treatment of human macrophages with brefeldin A. Human macrophages were treated with brefeldin A (2 μg/ml), a reagent that disrupts the Golgi, or vehicle for the indicated lengths of time. Cell lysates were separated by SDS-PAGE under reducing conditions, followed by immunoblotting with anti–TLR8-N mAb. The band intensity of FL-TLR8 was quantified using National Institutes of Health ImageJ software and normalized to that of tubulin. Results are expressed as fold intensity relative to the intensity of vehicle-treated cells.

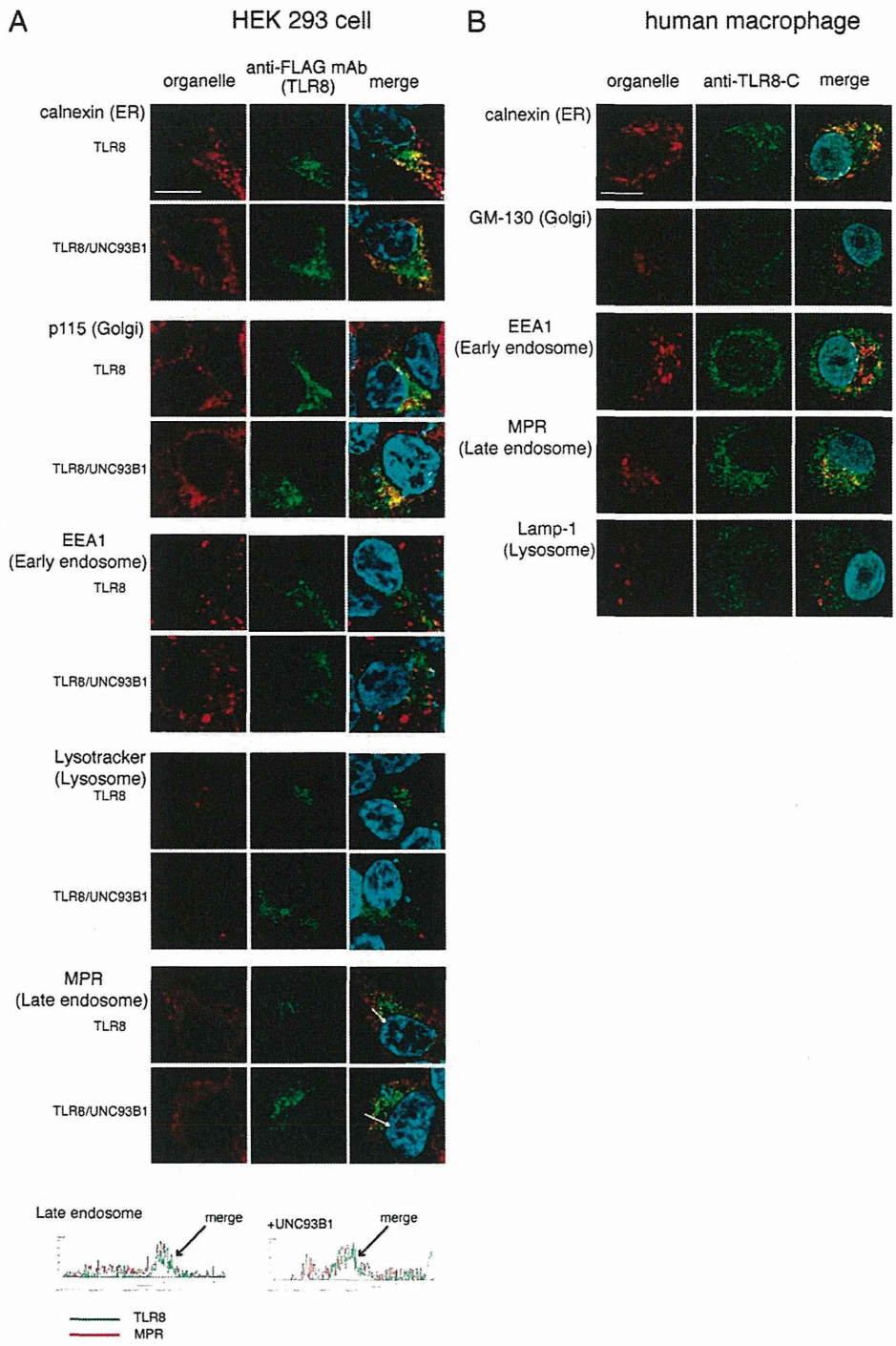

FIGURE 8. TLR8 localized to the early/late endosomes in human macrophages. (**A**) UNC93B1 facilitated intracellular trafficking of TLR8. HEK293 cells expressing FLAG-tagged hTLR8, with or without UNC93B1, were fixed, permeabilized, and stained with anti-FLAG mAb and the indicated pAbs against organelle marker proteins, followed by Alexa Fluor 488–labeled or Alexa Fluor 568–labeled secondary Ab. Red, organelle markers; green, TLR8; blue, DAPI-stained nuclei. Scale bar, 10 μm. Graphs display the measured fluorescence intensity along the white line in the merged panels of MPR and TLR8 with or without UNC93B1. (**B**) Subcellular localization of endogenous TLR8 in monocyte-derived macrophages. Macrophages were fixed, permeabilized, and stained with anti–TLR8-C pAb and the indicated mouse mAbs against organelle marker proteins, followed by Alexa Fluor 488–labeled or Alexa Fluor 568–labeled secondary Ab. Red, organelle markers; green, TLR8; blue, DAPI-stained nuclei. Scale bar, 10 μm.

TLR7 and TLR9 are closely associated with autoimmune disorders because of their expression in B cells and pDCs (52, 53). The relationship between TLR8 and autoimmune disorders was suggested in a TLR8-knockout mouse study that showed a pivotal role for mTLR8 in the regulation of TLR7 expression and prevention of spontaneous autoimmunity (54). In addition, a recent study using hTLR8-transgenic mice clearly demonstrated the connection between TLR8 and autoimmune inflammation (55). TLR8 was shown to induce proinflammatory cytokine production in response to microRNA within exosomes from tumor cells (38). In view of the unique expression profile and signaling skewed toward NF-κB activation, TLR8 might be involved in the development of inflammatory disorders in a distinct manner. Identification of endogenous and exogenous TLR8 ligands and their recognition mechanisms are important for a full understanding of the role of TLR8 in innate immunity and protection against undesirable inflammation and autoimmune responses.

Acknowledgments

We thank our laboratory members for valuable discussions. We also thank M. Nakai, R. Takemura, K. Mugikura, Y. Takeda, A. Maruyama, and K. Takashima for preparing blood cells. We also thank Dr. K. Miyake, Dr. S. Akira, and Dr. S. Nagata for providing the plasmids.

Disclosures

The authors have no financial conflicts of interest.

References

1. Medzhitov, R., and C. A. Janeway, Jr. 1997. Innate immunity: the virtues of a nonclonal system of recognition. *Cell* 91: 295–298.
2. Akira, S., S. Uematsu, and O. Takeuchi. 2006. Pathogen recognition and innate immunity. *Cell* 124: 783–801.
3. Barton, G. M., and J. C. Kagan. 2009. A cell biological view of Toll-like receptor function: regulation through compartmentalization. *Nat. Rev. Immunol.* 9: 535–542.
4. Matsumoto, M., K. Funami, M. Tanabe, H. Oshiumi, M. Shingai, Y. Seto, A. Yamamoto, and T. Seya. 2003. Subcellular localization of Toll-like receptor 3 in human dendritic cells. *J. Immunol.* 171: 3154–3162.
5. Latz, E., A. Schoenemeyer, A. Visintin, K. A. Fitzgerald, B. G. Monks, C. F. Knetter, E. Lien, N. J. Nilsen, T. Espevik, and D. T. Golenbock. 2004. TLR9 signals after translocating from the ER to CpG DNA in the lysosome. *Nat. Immunol.* 5: 190–198.
6. Tabeta, K., K. Hoebe, E. M. Janssen, X. Du, P. Georgel, K. Crozat, S. Mudd, N. Mann, S. Sovath, J. Goode, et al. 2006. The Unc93b1 mutation 3d disrupts exogenous antigen presentation and signaling via Toll-like receptors 3, 7 and 9. *Nat. Immunol.* 7: 156–164.
7. Brinkmann, M. M., E. Spooner, K. Hoebe, B. Beutler, H. L. Ploegh, and Y. M. Kim. 2007. The interaction between the ER membrane protein UNC93B and TLR3, 7, and 9 is crucial for TLR signaling. *J. Cell Biol.* 177: 265–275.
8. Kim, Y. M., M. M. Brinkmann, M. E. Paquet, and H. L. Ploegh. 2008. UNC93B1 delivers nucleotide-sensing toll-like receptors to endolysosomes. *Nature* 452: 234–238.
9. Fukui, R., S. Saitoh, F. Matsumoto, H. Kozuka-Hata, M. Oyama, K. Tabeta, B. Beutler, and K. Miyake. 2009. Unc93B1 biases Toll-like receptor responses to nucleic acid in dendritic cells toward DNA- but against RNA-sensing. *J. Exp. Med.* 206: 1339–1350.
10. Itoh, H., M. Tatematsu, A. Watanabe, K. Iwano, K. Funami, T. Seya, and M. Matsumoto. 2011. UNC93B1 physically associates with human TLR8 and regulates TLR8-mediated signaling. *PLoS ONE* 6: e28500.
11. Funami, K., M. Matsumoto, H. Oshiumi, T. Akazawa, A. Yamamoto, and T. Seya. 2004. The cytoplasmic 'linker region' in Toll-like receptor 3 controls receptor localization and signaling. *Int. Immunol.* 16: 1143–1154.
12. Nishiya, T., E. Kajita, S. Miwa, and A. L. Defranco. 2005. TLR3 and TLR7 are targeted to the same intracellular compartments by distinct regulatory elements. *J. Biol. Chem.* 280: 37107–37117.
13. Barton, G. M., J. C. Kagan, and R. Medzhitov. 2006. Intracellular localization of Toll-like receptor 9 prevents recognition of self DNA but facilitates access to viral DNA. *Nat. Immunol.* 7: 49–56.
14. Chuang, T.-H., and R. J. Ulevitch. 2000. Cloning and characterization of a sub-family of human toll-like receptors: hTLR7, hTLR8 and hTLR9. *Eur. Cytokine Netw.* 11: 372–378.
15. Du, X., A. Poltorak, Y. Wei, and B. Beutler. 2000. Three novel mammalian toll-like receptors: gene structure, expression, and evolution. *Eur. Cytokine Netw.* 11: 362–371.
16. Bell, J. K., G. E. D. Mullen, C. A. Leifer, A. Mazzoni, D. R. Davies, and D. M. Segal. 2003. Leucine-rich repeats and pathogen recognition in Toll-like receptors. *Trends Immunol.* 24: 528–533.
17. Latz, E., A. Verma, A. Visintin, M. Gong, C. M. Sirois, D. C. Klein, B. G. Monks, C. J. McKnight, M. S. Lamphier, W. P. Duprex, et al. 2007. Ligand-induced conformational changes allosterically activate Toll-like receptor 9. *Nat. Immunol.* 8: 772–779.
18. Hemmi, H., T. Kaisho, O. Takeuchi, S. Sato, H. Sanjo, K. Hoshino, T. Horiuchi, H. Tomizawa, K. Takeda, and S. Akira. 2002. Small anti-viral compounds activate immune cells via the TLR7 MyD88-dependent signaling pathway. *Nat. Immunol.* 3: 196–200.
19. Jurk, M., F. Heil, J. Vollmer, C. Schetter, A. M. Krieg, H. Wagner, G. Lipford, and S. Bauer. 2002. Human TLR7 or TLR8 independently confer responsiveness to the antiviral compound R-848. *Nat. Immunol.* 3: 499.
20. Heil, F., H. Hemmi, H. Hochrein, F. Ampenberger, C. Kirschning, S. Akira, G. Lipford, H. Wagner, and S. Bauer. 2004. Species-specific recognition of single-stranded RNA via toll-like receptor 7 and 8. *Science* 303: 1526–1529.
21. Diebold, S. S., T. Kaisho, H. Hemmi, S. Akira, and C. Reis e Sousa. 2004. Innate antiviral responses by means of TLR7-mediated recognition of single-stranded RNA. *Science* 303: 1529–1531.
22. Hemmi, H., O. Takeuchi, T. Kawai, T. Kaisho, S. Sato, H. Sanjo, M. Matsumoto, K. Hoshino, H. Wagner, K. Takeda, and S. Akira. 2000. A Toll-like receptor recognizes bacterial DNA. *Nature* 408: 740–745.
23. Krieg, A. M. 2002. CpG motifs in bacterial DNA and their immune effects. *Annu. Rev. Immunol.* 20: 709–760.
24. Matsumoto, F., S. Saitoh, R. Fukui, T. Kobayashi, N. Tanimura, K. Konno, Y. Kusumoto, S. Akashi-Takamura, and K. Miyake. 2008. Cathepsins are required for Toll-like receptor 9 responses. *Biochem. Biophys. Res. Commun.* 367: 693–699.
25. Ewald, S. E., B. L. Lee, L. Lau, K. E. Wickliffe, G. P. Shi, H. A. Chapman, and G. M. Barton. 2008. The ectodomain of Toll-like receptor 9 is cleaved to generate a functional receptor. *Nature* 456: 658–662.
26. Park, B., M. M. Brinkmann, E. Spooner, C. C. Lee, Y. M. Kim, and H. L. Ploegh. 2008. Proteolytic cleavage in an endolysosomal compartment is required for activation of Toll-like receptor 9. *Nat. Immunol.* 9: 1407–1414.
27. Sepulveda, F. E., S. Maschalidi, R. Colisson, L. Heslop, C. Ghirelli, E. Sakka, A. M. Lennon-Duménil, S. Amigorena, L. Cabanie, and B. Manoury. 2009. Critical role for asparagine endopeptidase in endocytic Toll-like receptor signaling in dendritic cells. *Immunity* 31: 737–748.
28. Ewald, S. E., A. Engel, J. Lee, M. Wang, M. Bogyo, and G. M. Barton. 2011. Nucleic acid recognition by Toll-like receptors is coupled to stepwise processing by cathepsins and asparagine endopeptidase. *J. Exp. Med.* 208: 643–651.
29. Maschalidi, S., S. Hässler, F. Blanc, F. E. Sepulveda, M. Tohme, M. Chignard, P. van Endert, M. Si-Tahar, D. Descamps, and B. Manoury. 2012. Asparagine endopeptidase controls anti-influenza virus immune responses through TLR7 activation. *PLoS Pathog.* 8: e1002841.
30. Hipp, M. M., D. Shepherd, U. Gileadi, M. C. Aichinger, B. M. Kessler, M. J. Edelmann, R. Essalmani, N. G. Seidah, C. Reis e Sousa, and V. Cerundolo. 2013. Processing of human toll-like receptor 7 by furin-like proprotein convertases is required for its accumulation and activity in endosomes. *Immunity* 39: 711–721.
31. Kanno, A., C. Yamamoto, M. Onji, R. Fukui, S. Saitoh, Y. Motoi, T. Shibata, F. Matsumoto, T. Muta, and K. Miyake. 2013. Essential role for Toll-like receptor 7 (TLR7)-unique cysteines in an intramolecular disulfide bond, proteolytic cleavage and RNA sensing. *Int. Immunol.* 25: 413–422.
32. Onji, M., A. Kanno, S. Saitoh, R. Fukui, Y. Motoi, T. Shibata, F. Matsumoto, A. Lamichhane, S. Sato, H. Kiyono, et al. 2013. An essential role for the N-terminal fragment of Toll-like receptor 9 in DNA sensing. *Nat. Commun.* 4: 1949.
33. Hornung, V., S. Rothenfusser, S. Britsch, A. Krug, B. Jahrsdörfer, T. Giese, S. Endres, and G. Hartmann. 2002. Quantitative expression of toll-like receptor 1-10 mRNA in cellular subsets of human peripheral blood mononuclear cells and sensitivity to CpG oligodeoxynucleotides. *J. Immunol.* 168: 4531–4537.
34. Peng, G., Z. Guo, Y. Kiniwa, K. S. Voo, W. Peng, T. Fu, D. Y. Wang, Y. Li, H. Y. Wang, and R. F. Wang. 2005. Toll-like receptor 8-mediated reversal of CD4+ regulatory T cell function. *Science* 309: 1380–1384.
35. Janke, M., J. Poth, V. Wimmenauer, T. Giese, C. Coch, W. Barchet, M. Schlee, and G. Hartmann. 2009. Selective and direct activation of human neutrophils but not eosinophils by Toll-like receptor 8. *J. Allergy Clin. Immunol.* 123: 1026–1033.
36. Jongbloed, S. L., A. J. Kassianos, K. J. McDonald, G. J. Clark, X. Ju, C. E. Angel, C. J. Chen, P. R. Dunbar, R. B. Wadley, V. Jeet, et al. 2010. Human CD141+ (BDCA-3)+ dendritic cells (DCs) represent a unique myeloid DC subset that cross-presents necrotic cell antigens. *J. Exp. Med.* 207: 1247–1260.
37. Sarvestani, S. T., B. R. Williams, and M. P. Gantier. 2012. Human Toll-like receptor 8 can be cool too: implications for foreign RNA sensing. *J. Interferon Cytokine Res.* 32: 350–361.
38. Fabbri, M., A. Paone, F. Calore, R. Galli, E. Gaudio, R. Santhanam, F. Lovat, P. Fadda, C. Mao, G. J. Nuovo, et al. 2012. MicroRNAs bind to Toll-like receptors to induce prometastatic inflammatory response. *Proc. Natl. Acad. Sci. USA* 109: E2110–E2116.
39. Tanji, H., U. Ohto, T. Shibata, K. Miyake, and T. Shimizu. 2013. Structural reorganization of the Toll-like receptor 8 dimer induced by agonistic ligands. *Science* 339: 1426–1429.
40. Zarember, K. A., and P. J. Godowski. 2002. Tissue expression of human Toll-like receptors and differential regulation of Toll-like receptor mRNAs in leukocytes in response to microbes, their products, and cytokines. *J. Immunol.* 168: 554–561.
41. Schmid, H., R. Sauerbrei, G. Schwarz, E. Weber, H. Kalbacher, and C. Driessen. 2002. Modulation of the endosomal and lysosomal distribution of cathepsins B, L and S in human monocytes/macrophages. *Biol. Chem.* 383: 1277–1283.
42. Matsumoto, M., and T. Seya. 2008. TLR3: interferon induction by double-stranded RNA including poly(I:C). *Adv. Drug Deliv. Rev.* 60: 805–812.
43. Garcia-Cattaneo, A., F. X. Gobert, M. Müller, F. Toscano, M. Flores, A. Lescure, E. Del Nery, and P. Benaroch. 2012. Cleavage of Toll-like receptor 3 by cathepsins B and H is essential for signaling. *Proc. Natl. Acad. Sci. USA* 109: 9053–9058.
44. Qi, R., D. Singh, and C. C. Kao. 2012. Proteolytic processing regulates Toll-like receptor 3 stability and endosomal localization. *J. Biol. Chem.* 287: 32617–32629.
45. Toscano, F., Y. Estornes, F. Virard, A. Garcia-Cattaneo, A. Pierrot, B. Vanbervliet, M. Bonnin, M. J. Ciancanelli, S. Y. Zhang, K. Funami, et al. 2013. Cleaved/associated TLR3 represents the primary form of the signaling receptor. *J. Immunol.* 190: 764–773.
46. Tatematsu, M., F. Nishikawa, T. Seya, and M. Matsumoto. 2013. Toll-like receptor 3 recognizes incomplete stem structures in single-stranded viral RNA. *Nat. Commun.* 4: 1833.
47. Li, Y., I. C. Berke, and Y. Modis. 2012. DNA binding to proteolytically activated TLR9 is sequence-independent and enhanced by DNA curvature. *EMBO J.* 31: 919–931.
48. Gringhuis, S. I., M. van der Vlist, L. M. van den Berg, J. den Dunnen, M. Litjens, and T. B. Geijtenbeek. 2010. HIV-1 exploits innate signaling by TLR8 and DC-SIGN for productive infection of dendritic cells. *Nat. Immunol.* 11: 419–426.
49. Han, X., X. Li, S. C. Yue, A. Anandaiah, F. Hashem, P. S. Reinach, H. Koziel, and S. D. Tachado. 2012. Epigenetic regulation of tumor necrosis factor α (TNFα) release in human macrophages by HIV-1 single-stranded RNA (ssRNA) is dependent on TLR8 signaling. *J. Biol. Chem.* 287: 13778–13786.
50. Saitoh, T., J. Komano, Y. Saitoh, T. Misawa, M. Takahama, T. Kozaki, T. Uehata, H. Iwasaki, H. Omori, S. Yamaoka, et al. 2012. Neutrophil extracellular traps mediate a host defense response to human immunodeficiency virus-1. *Cell Host Microbe* 12: 109–116.
51. Ablasser, A., H. Poeck, D. Anz, M. Berger, M. Schlee, S. Kim, C. Bourquin, N. Goutagny, Z. Jiang, K. A. Fitzgerald, et al. 2009. Selection of molecular structure and delivery of RNA oligonucleotides to activate TLR7 versus TLR8 and to induce high amounts of IL-12p70 in primary human monocytes. *J. Immunol.* 182: 6824–6833.

52. Marshak-Rothstein, A. 2006. Toll-like receptors in systemic autoimmune disease. *Nat. Rev. Immunol.* 6: 823–835.
53. Krieg, A. M., and J. Vollmer. 2007. Toll-like receptors 7, 8, and 9: linking innate immunity to autoimmunity. *Immunol. Rev.* 220: 251–269.
54. Demaria, O., P. P. Pagni, S. Traub, A. de Gassart, N. Branzk, A. J. Murphy, D. M. Valenzuela, G. D. Yancopoulos, R. A. Flavell, and L. Alexopoulou. 2010. TLR8 deficiency leads to autoimmunity in mice. *J. Clin. Invest.* 120: 3651–3662.
55. Guiducci, C., M. Gong, A.-M. Cepika, Z. Xu, C. Tripodo, L. Bennett, C. Crain, P. Quartier, J. J. Cush, V. Pascual, et al. 2013. RNA recognition by human TLR8 can lead to autoimmune inflammation. *J. Exp. Med.* 210: 2903–2919.
56. Kokkinopoulos, I., W. J. Jordan, and M. A. Ritter. 2005. Toll-like receptor mRNA expression patterns in human dendritic cells and monocytes. *Molec. Immunol.* 42: 957–968.

The International Journal of Biochemistry & Cell Biology 53 (2014) 329–333

Contents lists available at ScienceDirect

The International Journal of Biochemistry & Cell Biology

journal homepage: www.elsevier.com/locate/biocel

Cells in focus

Dendritic cell subsets involved in type I IFN induction in mouse measles virus infection models

Hiromi Takaki*, Hiroyuki Oshiumi, Misako Matsumoto, Tsukasa Seya*

Department of Microbiology and Immunology, Hokkaido University Graduate School of Medicine, Kita-ku, Sapporo 060-8638, Japan

ARTICLE INFO

Article history:
Received 20 March 2014
Received in revised form 28 April 2014
Accepted 1 May 2014
Available online 4 June 2014

Keywords:
Dendritic cells
Measles virus
Mouse model
Type I interferon (IFN)
Immune suppression

ABSTRACT

Measles caused by measles virus (MV) infection remains important in child mortality. Although the natural host of MV is human, mouse models expressing MV entry receptors (human CD46, CD150) and disrupting the interferon (IFN) pathways work for investigating immune responses during early MV infection *in vivo*. Dendritic cells (DCs) are primary targets for MV in the mouse models and are efficiently infected with several MV strains in the respiratory tract *in vivo*. However, questions remain about what kind of DC in a variety of DC subsets is involved in initial MV infection and how the RNA sensors evoke circumventing signals against MV in infected DCs. Since type I IFN-inducing pathways are a pivotal defense system that leads to the restriction of systemic viral infection, we have generated CD150-transgenic mice with disrupting each of the IFN-inducing pathway, and clarified that DC subsets had subset-specific IFN-inducing systems, which critically determined the DC's differential susceptibility to MV.

1. Introduction

The pathogenic measles virus (MV) causes measles in infants. The MV genome is a nonsegmented negative single-stranded RNA consisting of six genes that encode the nucleocapsid (N), phosphoprotein (P), matrix (M), fusion (F), hemagglutinin (H), and large (L) proteins. The P gene encodes P protein and the nonstructural V and C proteins. Although the nonstructural V and C proteins of wild type (WT) strains of MV are important in suppressing the host interferon (IFN) response in human cells (Gerlier and Valentin, 2009), WT strains of MV are less able to suppress type I IFN production in murine cells than in human cells (Shingai et al., 2005), suggesting that V and C proteins are relatively ineffective suppressors for IFN response in murine cells.

CD46 (also called MCP) was first identified as an MV entry receptor for laboratory-adapted and vaccine strains of MV. CD46 is expressed in all human nucleated cells including epithelial cells (Gerlier and Valentin, 2009). In 2000, human CD150, a signaling lymphocyte activation molecule (SLAM), was identified as the second MV entry receptor for all MV strains including WT (Tatsuo et al., 2000). Expression of CD150 is restricted to activated lymphocytes, dendritic cells (DCs), and macrophages (Delpeut et al., 2012), consistent with the lymphotropism of MV. However, the expression pattern of CD150 does not explain why WT strains of MV infect epithelial cells that do not express CD150. Recently, human nectin-4 (also called poliovirus receptor-related 4, PVRL4) was identified as the third entry receptor for WT strains of MV (Mühlebach et al., 2011; Noyce et al., 2011). Expression of nectin-4 is restricted to the basolateral surface of epithelial cells (Delpeut et al., 2012). Thus, laboratory-adapted and vaccine strains of MV use CD46 and CD150 as entry receptors, and WT strains of MV use CD150 and nectin-4. Initial infection with WT stains of MV *via* CD150 occurs in DCs and alveolar macrophages (AMs) and secondary spreading of MV infection is established in lymphocytes through infected DCs and AMs. Ultimately, MV-infected lymphocytes systemically spread to distal sites including the respiratory tract and then MV infects epithelial cells *via* nectin-4, resulting in release of MV into the airway lumen of the infected lung (Delpeut et al., 2012). C-type lectin DC-SIGN (also called CD209) has an important role for infection of DCs by laboratory-adapted and WT strains of MV (de Witte et al., 2006), although DC-SIGN is dispensable for MV entry. Both attachment and infection of immature DCs with MV are blocked by DC-SIGN inhibitors, suggesting that DC-SIGN is critical for enhancement of CD46/CD150-mediated infection of DCs (de Witte et al., 2006).

Human CD150 transgenic (Tg) and CD150 knock-in mice were generated as MV infection models to study receptor tropism and the immune dynamics of MV (Hahm et al., 2003, 2004; Ohno et al., 2007; Sellin et al., 2006; Shingai et al., 2005; Welstead et al., 2005) and these mice were somehow permissive to MV *in vivo*.

* Corresponding authors at: Department of Microbiology and Immunology, Hokkaido University Graduate School of Medicine, Kita 15, Nishi 7, Kita-ku, Sapporo 060-8638, Japan. Tel.: +81 11 706 7866; fax: +81 11 706 7866.
E-mail addresses: tahiromi@sci.hokudai.ac.jp (H. Takaki), seya-tu@pop.med.hokudai.ac.jp (T. Seya).

http://dx.doi.org/10.1016/j.biocel.2014.05.001
1357-2725/

Systemic infection by WT strains of MV *in vivo* was observed in CD150Tg/*Ifnar*$^{-/-}$ mice, generated by crossing CD150Tg mice with mice having the disrupted IFN receptor 1 (*Ifnar*) gene; the other is CD150Tg/*Stat1*$^{-/-}$ mice, generated by crossing CD150Tg mice with mice knocked out for the signal transduction and activator of transcription 1 (*Stat1*) gene, which is a major signaling molecule for the IFN receptor (Shingai et al., 2005; Welstead et al., 2005). Both models indicate the importance of the IFNAR pathway for restricting MV *in vivo* infection in mice. DCs and AMs are primary targets for MV intranasally inoculated into CD150Tg models (Ferreira et al., 2010), since these cells express CD150 and are located in the lung where host cells firstly encounter MV. Results from mouse models for MV *in vivo* infection reflect *in vitro* high susceptibility of human monocyte-derived DCs (moDCs) to MV. DCs and AMs are the first target cells during early MV infection in monkeys (de Swart et al., 2007; Lemon et al., 2011). All these data indicate that type I IFN produced by DCs and AMs primarily protects hosts from systemic MV infection.

In this review, we summarized the mouse model studies on the host antiviral response to MV infection, which involves both toll-like receptors (TLRs) and retinoic acid-inducible gene (RIG)-I-like receptors (RLRs) in specific DC subsets.

2. Type I IFN-inducing pathways respond to viral RNA

The IFN response, which is the induction of type I IFN-α/β is a major antiviral defense pathway that confers virus resistance to neighboring cells. Previous reports showed that viral RNA is detected by cytoplasmic pattern recognition receptors (PRRs) such as RIG-I and the melanoma differentiation-associated gene 5 (MDA5) (Kawai and Akira, 2009). MDA5 and RIG-I detect long and short dsRNA, respectively (Kato et al., 2008). TLR3 recognizes extracellular double-stranded RNA (dsRNA) in the endosome whereas RIG-I and MDA5 sense cytoplasmic dsRNA (Fig. 1). TLR3 recruits the adaptor, Toll/interleukin-1 receptor (TIR) homology domain-containing adaptor molecule 1 (TICAM-1, also called TRIF) in response to dsRNA and induces type I IFN production. Activation of RLRs is regulated by multiple consecutive processes including dephosphorylation, ubiquitination and oligomerization of RLR (Gack et al., 2007; Wies et al., 2013). The CARD domain of RLRs is phosphorylated by unknown kinases in steady state, prohibiting RLR activation (Wies et al., 2013). Viral infection activates RLRs *via* dephosphorylation by serine–threonine phosphatases PP1α and PP1γ (Wies et al., 2013). The dephosphorylated RLRs provide signals through the mitochondrial antiviral signaling protein (MAVS; also called VISA, Cardif, or IPS-1) to induce type I IFN. Disrupting these adaptor genes results in failure to activate IFN regulatory factor (IRF)-3 and IRF-7, abrogating type I IFN production and antiviral host defense. Virus-derived single-stranded RNA (ssRNA) is recognized by TLR7 and TLR8 which are in the endosome. MyD88-dependent signaling is activated upon viral RNA recognition by TLR7 to induce type I IFNs (Kawai and Akira, 2009). Unlike ubiquitous RLRs, TLR expression is restricted to particular cell types with a different set of TLRs (Table 1) (Edwards et al., 2003). This differential expression pattern of TLRs directs specific sets of cells to respond to particular TLR ligands, which enhance a variety of immune responses.

3. Type I IFN induction in MV-infected murine DCs

Studies in mice with targeted gene deletions provide insight into the mechanisms of type I IFN induction in response to MV infection *in vivo* and *in vitro*. Bone marrow-derived DCs (BMDCs) were used to study MV permissiveness of DCs, initially in CD150Tg mice (Ohno et al., 2007; Shingai et al., 2005; Welstead et al., 2005). Studies using BMDCs from CD150Tg mice in combination with *Mavs*$^{-/-}$, *Irf3*$^{-/-}$/*Irf7*$^{-/-}$, *Ticam1*$^{-/-}$ and *Myd88*$^{-/-}$ mice showed that type I IFN expression in BMDCs completely relied on MAVS but not TICAM-1 and MyD88 (Takaki et al., 2014). Surprisingly, BMDCs derived from CD150Tg/*Irf3*$^{-/-}$/*Irf7*$^{-/-}$ mice produce a detectable IFN-β in response to MV infection, which confers nonpermissiveness to CD150Tg/*Irf3*$^{-/-}$/*Irf7*$^{-/-}$ BMDCs (Takaki et al., 2014). A pharmacological study indicated that MV-derived IFN-β expression partially depended on NF-κB (Takaki et al., 2014). A recent study using West Nile virus showed that IRF3/IRF7 and IRF5 coordinately regulate the type I IFN response in DCs (Lazear et al., 2013). For MV, IRF5 might be a transcription factor for MAVS-dependent and IRF3/IRF7-independent type I IFN induction in BMDCs (Fig. 2).

An *in vivo* MV infection study using a CD150Tg mouse model revealed that MAVS disruption scarcely led MV permissiveness or type I IFN gene expression in the spleen compared to CD150Tg mice (Takaki et al., 2013). *In vitro* infection assays showed that isolated cell subsets of CD11c^{+} DCs, but not T or B cells, mainly produced type I IFN in response to MV infection through a MAVS-independent pathway. Various types of DCs have been identified in mouse secondary lymphoid tissues, including three CD11c^{high} subsets of conventional DCs (cDCs): CD8α^{+}, CD4^{+} and CD4^{-} CD8α^{-} double negative (DN) DCs (Vremec et al., 2000), and one subset of CD11c^{low} plasmacytoid DCs (pDCs) (Asselin-Paturel et al., 2001). These DC subsets express different sets of TLR genes and have distinct functions (Table 1) (Edwards et al., 2003; Luber et al., 2010). Mouse pDCs express most TLRs except TLR3 and therefore respond to a wide range of pathogen-associated molecular patterns including TLR7 ligand (Boonstra et al., 2003; Edwards et al., 2003). CD8α^{+} DCs express high amounts of TLR3, but not TLR7 (Edwards et al., 2003) and mainly participate in poly I:C-induced cross-presentation. Although a CD4^{+} and DN DCs have a similar TLR expression pattern (Edwards et al., 2003), CD4^{+} DCs but not DN DCs express TLR7 protein at low levels (Takaki et al., 2013). Type I IFN expression is induced in CD4^{+} DCs and pDCs, but not CD8α^{+} and DN DCs that are isolated from MAVS-disrupted mice during *in vitro* MV infection (Takaki et al., 2013). This result indicates that type I IFN-inducing pathways in pDC and CD4^{+} DCs are independent of the MAVS pathway. A pharmacological study showed that the MyD88 pathway is involved in a MAVS-independent type I IFN-inducing pathway (Takaki et al., 2013). This result was confirmed using CD150Tg/*Myd88*$^{-/-}$ pDCs, suggesting that TLR7 is responsible for recognition of MV RNA in CD4^{+} and pDCs. Since the RLR-MAVS pathway usually senses endogenous viral RNA in CD4^{+} DCs (Luber et al., 2010), MAVS disruption highlights that the MyD88 pathway participates in initial type I IFN induction in CD4^{+} DCs in MV infection (Fig. 2). However, CD150Tg/*Myd88*$^{-/-}$ mice are not permissive to MV infection *in vivo*, both MyD88 in pDCs and CD4^{+} DCs and MAVS in other cells contribute to protection against systemic MV infection.

Since TLR7 is in the endosome, viral RNA transport to the endosome is required to activate the TLR7/MyD88 pathway. Autophagy is required for the recognition of vesicular stomatitis virus by TLR7 to transport cytosolic viral replication intermediates into the lysosome, leading to type I IFN production in pDCs (Lee et al., 2007) IFN-β mRNA expression is induced in UV-irradiated MV-infected CD150Tg/*Mavs*$^{-/-}$ DCs; however, treatment with an autophagy inhibitor prevented this IFN-β induction (unpublished data). These data suggest that autophagy but not viral replication is required for MV-mediated type I IFN induction *via* TLR7 in MAVS-disrupted murine DCs.

In contrast to BMDCs, type I IFN gene expression is observed in DCs and splenocytes derived from MV-infected CD150Tg/*Mavs*$^{-/-}$ mice, which prevents DCs from MV infection *in vivo* in these mice (Takaki et al., 2013, 2014). RIG-I/MAVS but not TLR7/MyD88 mediates the antiviral response to RNA virus in conventional DCs. The

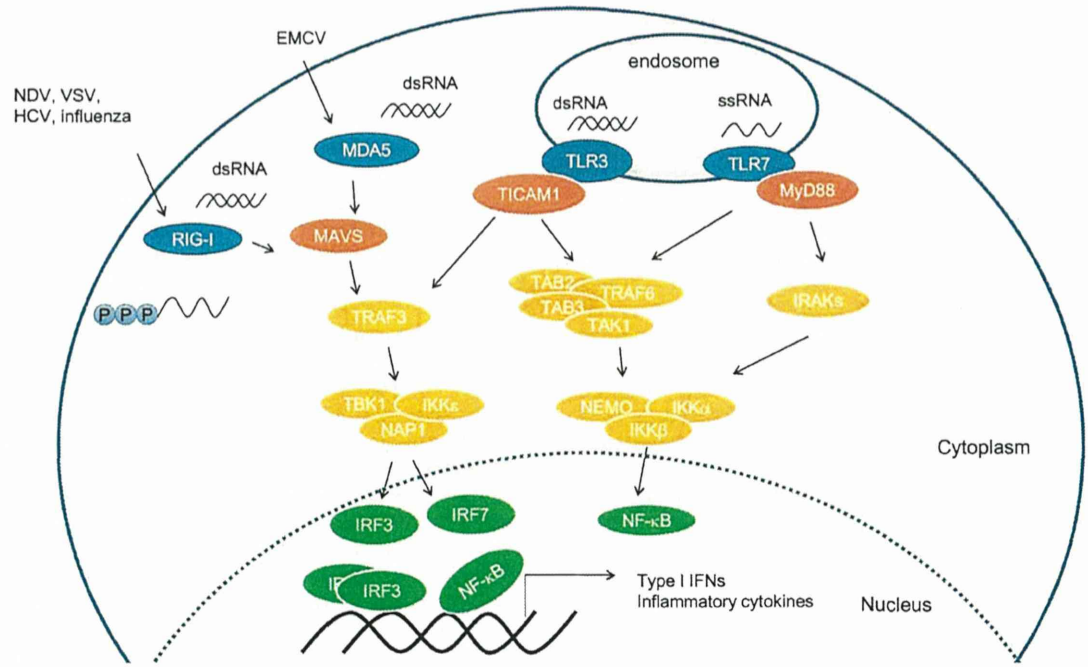

Fig. 1. Recognition of RNA by RLRs and TLRs. Double-stranded RNA (dsRNA) synthesized by RNA virus replication in infected cells is recognized by endosomal TLR3 and cytosolic RIG-I like receptors (RLRs), RIG-I and MDA5. They differentially recognize viral dsRNA products such that long dsRNA chains fit in MDA5, 5′-triphosphates short dsRNA couple with RIG-I and structured RNA activate TLR3 (Tatematsu et al., 2013). The outline of their signaling cascades that lead to the activation of IRF3 and NF-κB is overviewed (Kawai and Akira, 2009). Single-stranded RNA (ssRNA) is recognized by endosomal TLR7, leading to the activation of NF-κB and IKK α/β *via* adaptor protein MyD88. Transcription factor activation resuls in expression of type I IFN and inflammatory cytokines. NDV, newcastle disease virus; SeV, sendai virus; HCV, hepatitis C; EMCV, encephalomyocarditis virus

Table 1
Expression of TLRs in murine and human DC subset.

			TLR1	TLR2	TLR3	TLR4	TLR5	TLR6	TLR7	TLR8	TLR9	TLR10
Mouse	Conventional DCs ($CD11c^{high}$ $B220^-$)	$CD4^+$	+	+	–	+	+	+	+	–	+	–
		$CD4^-CD8\alpha^-$	+	+	+/–	+	+	+	+/–	–	+	–
		$CD4^-$	+	+	+	+	–	+	–	–	+	–
	Plasmacytoid DCs ($CD11c^{low}$ $B220^+$ $PDCA-1^+$)		+	+	–	+	+/–	+	+	–	+	–
Human	Myeloid DCs ($CD11c^+$)		+	+	+	+	+	+	+	+/–	–	+
	Monocyte-derived DCs (moDCs)		+	+	+	+	+	+/–	+/–	+	–	–
	Plasmacytoid DCs ($CD11c^-$ $BDCA2^+$ $BDCA4^+$)		+/–	–	–	–	–	–	+	–	+	+

TLR expression in murine and human DC subset is described in refs (Jarrossay et al., 2001; Kadowaki et al., 2001; Edwards et al., 2003; Luber et al., 2010).

studies using reporter mouse that expresses green fluorescence protein (GFP) under the control of the *Ifn-α6* promoter show that intranasal infection with newcastle disease virus (NDV) induces GFP expression in AMs and cDCs in lung as an initial defense *via* the RLR pathway (Kumagai et al., 2007). Although systemic NDV infection leads to GFP expression in not only pDCs but also cDCs and AMs, the frequency of GFP positive cells is higher in pDCs than in other cells. Thus, the activation of different subsets of DCs would be important to produce type I IFNs in systemic and local RNA virus infection.

Similar to murine DCs, PRRs expression differs with subsets of human DCs (Table 1) (Jarrossay et al., 2001; Kadowaki et al., 2001). In cDCs, MV transcription is required to activate type I IFN response, since UV-irradiated MV is unable to promote IFN-β production (Duhen et al., 2010). Type I IFN induction by pDCs depends on the recognition of MV RNA *via* the endosomal pathway, since UV-irradiated MV infection induces IFN-α production and this induction is cancelled by an endosomal acidification inhibitor in pDCs (Duhen et al., 2010). Although MV can inhibit TLR7 and TLR9-mediated type I IFN induction by MV-V and MV-C proteins in human pDCs (Pfaller and Conzelmann, 2008; Schlender et al., 2005; Yamaguchi et al., 2014), it remains unknown whether MV proteins act as suppressors in murine DCs. Moreover, MV interacts with human DC-SIGN to enhance infection of human DCs (de Witte et al., 2006). However, how MV-H protein binds murine CIRE/DC-SIGN is unknown. The findings in murine DCs may differ from those in human DCs when infected with MV.

4. Type I IFN and cytokines in the context of MV immunosuppression

DCs contribute to MV-induced immunosuppression, including downregulation of costimulatory molecules and inhibition of IL-12 production following lipopolysaccharide stimulation (Coughlin et al., 2013; Hahm et al., 2004, 2007). MV infection suppressed BMDCs development *via* type I IFN that acts through STAT2-dependent signaling but independent of the STAT1 signaling (Hahm et al., 2005). Furthermore, *in vivo* MV infection induces a T helper type 2 response, enhances apoptosis, and induces regulatory T cells (Koga et al., 2010; Sellin et al., 2009). Blocking IL-10 signaling prevents MV-induced immunosuppression in CD150 knock-in mice, indicating that IL-10 participates in immunosuppression (Koga et al., 2010). In addition, high amounts of IL-10 are produced in $CD4^+$ T cells obtained from MV-infected CD150Tg mice (Takaki

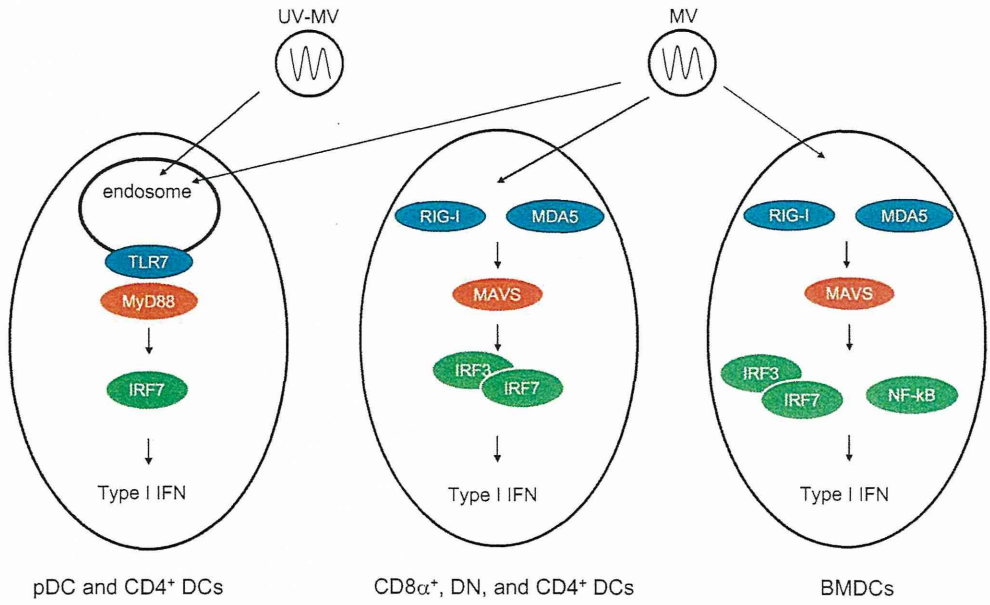

Fig. 2. Recognition of MV RNA in mouse DC subsets. DC subsets have their own viral RNA sensors to induce type I IFN. MV specifically infects these DC subsets. The ways for IFN induction in each DC subset are shown schematically. UV-MV; UV-irradiated MV

et al., 2014). In early infection by lymphocytic choriomeningitis virus (LCMV), type I IFN is produced *via* the TLR7/MyD88 pathway in pDCs. MDA5/MAVS-mediated type I IFN induction in other cells is required for sustained type I IFN responses to acute and chronic LCMV infection (Wang et al., 2012). Thus, different sources of type I IFN and signaling pathways affect immune responses to viral infection. Besides IL-10, IL-12 and type I IFN, other cytokines and signaling molecules affect MV-mediated immunomodulation. Further analysis is needed to clarify the function of DCs that modulate MV-induced immunosuppression.

Acknowledgements

We are grateful to Dr. M. Takeda (National Institute of Infectious Diseases, Japan) for fruitful discussions. This work was supported in part by Grants-in-Aid from the Ministry of Education, Science, and Culture (Specified Project for 'Carcinogenic Spiral') and the Ministry of Health, Labor, and Welfare of Japan, and by the Program of Founding Research Centers for Emerging and Reemerging Infectious Diseases (Host factors determining tropism and pathogenicity of zoonoses in association with innate immune system) and Japan Society for the promotion of Science Fellows (21-1368).

References

Asselin-Paturel C, Boonstra A, Dalod M, Durand I, Yessaad N, Dezutter-Dambuyant C, et al. Mouse type I IFN-producing cells are immature APCs with plasmacytoid morphology. Nat Immunol 2001;2:1144–50.

Boonstra A, Asselin-Paturel C, Gilliet M, Crain C, Trinchieri G, Liu YJ, et al. Flexibility of mouse classical and plasmacytoid-derived dendritic cells in directing T helper type 1 and 2 cell development: dependency on antigen dose and differential toll-like receptor ligation. J Exp Med 2003;197:101–9.

Coughlin MM, Bellini WJ, Rota PA. Contribution of dendritic cells to measles virus induced immunosuppression. Rev Med Virol 2013;23:126–38.

de Swart RL, Ludlow M, de Witte L, Yanagi Y, van Amerongen G, McQuaid S, et al. Predominant infection of CD150+ lymphocytes and dendritic cells during measles virus infection of macaques. PLoS Pathog 2007;3:e178.

de Witte L, Abt M, Schneider-Schaulies S, van Kooyk Y, Geijtenbeek TB. Measles virus targets DC-SIGN to enhance dendritic cell infection. J Virol 2006;80:3477–86.

Delpeut S, Noyce RS, Siu RW, Richardson CD. Host factors and measles virus replication. Curr Opin Virol 2012;2:773–83.

Duhen T, Herschke F, Azocar O, Druelle J, Plumet S, Delprat C, et al. Cellular receptors, differentiation and endocytosis requirements are key factors for type I IFN response by human epithelial, conventional and plasmacytoid dendritic infected cells by measles virus. Virus Res 2010;152:115–25.

Edwards AD, Diebold SS, Slack EM, Tomizawa H, Hemmi H, Kaisho T, et al. Toll-like receptor expression in murine DC subsets: lack of TLR7 expression by CD8 alpha+ DC correlates with unresponsiveness to imidazoquinolines. Eur J Immunol 2003;33:827–33.

Ferreira CS, Frenzke M, Leonard VH, Welstead GG, Richardson CD, Cattaneo R. Measles virus infection of alveolar macrophages and dendritic cells precedes spread to lymphatic organs in transgenic mice expressing human signaling lymphocytic activation molecule (SLAM, CD150). J Virol 2010;84:3033–42.

Gack MU, Shin YC, Joo CH, Urano T, Liang C, Sun L, et al. TRIM25 RING-finger E3 ubiquitin ligase is essential for RIG-I-mediated antiviral activity. Nature 2007;446:916–20.

Gerlier D, Valentin H. Measles virus interaction with host cells and impact on innate immunity. Curr Top Microbiol Immunol 2009;329:163–91.

Hahm B, Arbour N, Naniche D, Homann D, Manchester M, Oldstone MB. Measles virus infects and suppresses proliferation of T lymphocytes from transgenic mice bearing human signaling lymphocytic activation molecule. J Virol 2003;77:3505–15.

Hahm B, Arbour N, Oldstone MB. Measles virus interacts with human SLAM receptor on dendritic cells to cause immunosuppression. Virology 2004;323:292–302.

Hahm B, Cho JH, Oldstone MB. Measles virus-dendritic cell interaction via SLAM inhibits innate immunity: selective signaling through TLR4 but not other TLRs mediates suppression of IL-12 synthesis. Virology 2007;358:251–7.

Hahm B, Trifilo MJ, Zuniga EI, Oldstone MB. Viruses evade the immune system through type I interferon-mediated STAT2-dependent, but STAT1-independent, signaling. Immunity 2005;22:247–57.

Jarrossay D, Napolitani G, Colonna M, Sallusto F, Lanzavecchia A. Specialization and complementarity in microbial molecule recognition by human myeloid and plasmacytoid dendritic cells. Eur J Immunol 2001;31:3388–93.

Kadowaki N, Ho S, Antonenko S, Malefyt RW, Kastelein RA, Bazan F, et al. Subsets of human dendritic cell precursors express different toll-like receptors and respond to different microbial antigens. J Exp Med 2001;194:863–9.

Kato H, Takeuchi O, Mikamo-Satoh E, Hirai R, Kawai T, Matsushita K, et al. Length-dependent recognition of double-stranded ribonucleic acids by retinoic acid-inducible gene-I and melanoma differentiation-associated gene 5. J Exp Med 2008:1601–10, J205.

Kawai T, Akira S. The roles of TLRs, RLRs and NLRs in pathogen recognition. Int Immunol 2009;21:317–37.

Koga R, Ohno S, Ikegame S, Yanagi Y. Measles virus-induced immunosuppression in SLAM knock-in mice. J Virol 2010;84:5360–7.

Kumagai Y, Takeuchi O, Kato H, Kumar H, Matsui K, Morii E, et al. Alveolar macrophages are the primary interferon-alpha producer in pulmonary infection with RNA viruses. Immunity 2007;27:240–52.

Lazear HM, Lancaster A, Wilkins C, Suthar MS, Huang A, Vick SC, et al. IRF-3, IRF-5, and IRF-7 coordinately regulate the type I IFN response in myeloid dendritic cells downstream of MAVS signaling. PLoS Pathog 2013;9:e1003118.

Lee HK, Lund JM, Ramanathan B, Mizushima N, Iwasaki A. Autophagy-dependent viral recognition by plasmacytoid dendritic cells. Science 2007;315:1398–401.

Lemon K, de Vries RD, Mesman AW, McQuaid S, van Amerongen G, Yüksel S, et al. Early target cells of measles virus after aerosol infection of non-human primates. PLoS Pathog 2011;7:e1001263.
Luber CA, Cox J, Lauterbach H, Fancke B, Selbach M, Tschopp J, et al. Quantitative proteomics reveals subset-specific viral recognition in dendritic cells. Immunity 2010;32:279–89.
Mühlebach MD, Mateo M, Sinn PL, Prüfer S, Uhlig KM, Leonard VH, et al. Adherens junction protein nectin-4 is the epithelial receptor for measles virus. Nature 2011;480:530–3.
Noyce RS, Bondre DG, Ha MN, Lin LT, Sisson G, Tsao MS, et al. Tumor cell marker PVRL4 (nectin 4) is an epithelial cell receptor for measles virus. PLoS Pathog 2011;7:e1002240.
Ohno S, Ono N, Seki F, Takeda M, Kura S, Tsuzuki T, et al. Measles virus infection of SLAM (CD150) knockin mice reproduces tropism and immunosuppression in human infection. J Virol 2007;81:1650–9.
Pfaller CK, Conzelmann KK. Measles virus V protein is a decoy substrate for IkappaB kinase alpha and prevents Toll-like receptor 7/9-mediated interferon induction. J Virol 2008;82:12365–73.
Schlender J, Hornung V, Finke S, Günthner-Biller M, Marozin S, Brzózka K, et al. Inhibition of toll-like receptor 7- and 9-mediated alpha/beta interferon production in human plasmacytoid dendritic cells by respiratory syncytial virus and measles virus. J Virol 2005;79:5507–15.
Sellin CI, Davoust N, Guillaume V, Baas D, Belin MF, Buckland R, et al. High pathogenicity of wild-type measles virus infection in CD150 (SLAM) transgenic mice. J Virol 2006;80:6420–9.
Sellin CI, Jégou JF, Renneson J, Druelle J, Wild TF, Marie JC, et al. Interplay between virus-specific effector response and Foxp3 regulatory T cells in measles virus immunopathogenesis. PLoS ONE 2009;4:e4948.
Shingai M, Inoue N, Okuno T, Okabe M, Akazawa T, Miyamoto Y, et al. Wild-type measles virus infection in human CD46/CD150-transgenic mice: CD11c-positive dendritic cells establish systemic viral infection. J Immunol 2005;175:3252–61.
Takaki H, Honda K, Atarashi K, Kobayashi F, Ebihara T, Oshiumi H, et al. MAVS-dependent IRF3/7 bypass of interferon β-induction restricts the response to measles infection in CD150Tg mouse bone marrow-derived dendritic cells. Mol Immunol 2014;57:100–10.
Takaki H, Takeda M, Tahara M, Shingai M, Oshiumi H, Matsumoto M, et al. The MyD88 pathway in plasmacytoid and CD4+ dendritic cells primarily triggers Type I IFN production against measles virus in a mouse infection model. J Immunol 2013;191:4740–7.
Tatematsu M, Nishikawa F, Seya T, Matsumoto M. Toll-like receptor 3 recognizes incomplete stem structures in single-stranded viral RNA. Nat Commun 2013;4:1833.
Tatsuo H, Ono N, Tanaka K, Yanagi YSLAM. (CDw150) is a cellular receptor for measles virus. Nature 2000;406:893–7.
Vremec D, Pooley J, Hochrein H, Wu L, Shortman K. CD4 and CD8 expression by dendritic cell subtypes in mouse thymus and spleen. J Immunol 2000;164:2978–86.
Wang Y, Swiecki M, Cella M, Alber G, Schreiber RD, Gilfillan S, et al. Timing and magnitude of type I interferon responses by distinct sensors impact CD8T cell exhaustion and chronic viral infection. Cell Host Microbe 2012;11:631–42.
Welstead GG, Iorio C, Draker R, Bayani J, Squire J, Vongpunsawad S, et al. Measles virus replication in lymphatic cells and organs of CD150 (SLAM) transgenic mice. Proc Natl Acad Sci U S A 2005;102:16415–20.
Wies E, Wang MK, Maharaj NP, Chen K, Zhou S, Finberg RW, et al. Dephosphorylation of the RNA sensors RIG-I and MDA5 by the phosphatase PP1 is essential for innate immune signaling. Immunity 2013;38:437–49.
Yamaguchi M, Kitagawa Y, Zhou M, Itoh M, Gotoh B. An anti-interferon activity shared by paramyxovirus C proteins: inhibition of toll-like receptor 7/9-dependent alpha interferon induction. FEBS Lett 2014;588:28–34.

VIRAL IMMUNOLOGY
Volume 27, Number 6, 2014

Pp. 285–294
DOI: 10.1089/vim.2013.0140

The J6JFH1 Strain of Hepatitis C Virus Infects Human B-Cells with Low Replication Efficacy

Masato Nakai,[1,2] Tsukasa Seya,[1] Misako Matsumoto,[1] Kunitada Shimotohno,[3] Naoya Sakamoto,[2] and Hussein H. Aly[1,*]

Abstract

Hepatitis C virus (HCV) infection is a serious health problem worldwide that can lead to hepatocellular carcinoma or end-stage liver disease. Current treatment with pegylated interferon, ribavirin, and NS3/4A protease inhibitor would lead to a good prognosis in a large population of patients, but there is still no effective vaccine for HCV. HCV robustly infects hepatocytes in the liver. However, extrahepatic manifestations such as mixed cryoglobulinemia, a systemic immune complex-mediated disorder characterized by B-cell proliferation, which may evolve into overt B-cell non-Hodgkin's lymphoma, have been demonstrated. HCV-RNA is often found to be associated with peripheral blood lymphocytes, suggesting a possible interaction with peripheral blood mononuclear cells (PBMCs), especially B-cells with HCV. B-cell HCV infection was a matter of debate for a long time, and the new advance in HCV *in vitro* infectious systems suggest that exosome can transmit HCV genome to support "infection." We aimed to clarify the susceptibility of primary B-cells to HCV infection, and to study its functional effect. In this article, we found that the recombinant HCV J6JFH1 strain could infect human B-cells isolated from the peripheral blood of normal volunteers by the detection of both HCV-negative-strand RNA by reverse transcription polymerase chain reaction, and NS5A protein. We also show the blocking of HCV replication by type I interferon after B-cell HCV infection. Although HCV replication in B-lymphocytes showed lower efficiency, in comparison with hepatocyte line (Huh7) cells, our results clearly demonstrate that human B-lymphocytes without other non-B-cells can actually be infected with HCV, and that this interaction leads to the induction of B-cells' innate immune response, and change the response of these cells to apoptosis.

Introduction

CHRONIC INFECTION BY HEPATITIS C VIRUS (HCV) is the major cause of liver cirrhosis and hepatocellular carcinoma. About 3.1% of the global population is infected with HCV (50). Historically, a combination therapy with pegylated interferon (IFN) and ribavirin was used for patients infected with genotype 1 HCV. NS3/4A protease inhibitors were recently developed in addition to pegylated IFN and ribavirin, and their combinations have been clinically tried for HCV treatment since then. Although >70% of patients with high viral loads of HCV genotype 1b have a sustained viral response by the therapy using simeprevir or telaplevir with pegylated IFN and ribavirin (17,22), the remaining patients fail to eliminate the virus, and drug resistance remains an issue that must be resolved. Recent development of direct-acting antiviral (DAA) drugs (such as daclatasvir, asunaprevir, and sofosbuvir) are a promising therapeutic option beyond IFN in the treatment of HCV patients (6,32).

HCV is a single-stranded, positive-sense RNA virus in the Hepacivirus genus of the Flaviviridae family. Although HCV is known to infect hepatocytes in the liver and induce hepatitis *in vivo*, *in vitro* cultured primary hepatocytes barely support the HCV life cycle: only hepatoma Huh7 cells and its subclones can efficiently maintain the HCV life cycle of a very limited number of HCV strains *in vitro* (53).

Chronic hepatitis patients with HCV sometimes show other extrahepatic complications such as lymphoproliferative diseases (LPD), including cryoglobulinemia and B-cell malignant lymphoma, autoimmune diseases, and dermatitis (1,12,15,16). Epidemiological analysis shows that chronic HCV patients have higher rates of LPDs than non-HCV-infected populations (36,48,52). Several reports suggested that some lymphotropic HCV strains effectively infected human

Departments of [1]Microbiology and Immunology, and [2]Gastroenterology, Hokkaido University Graduate School of Medicine, Kita-ku, Japan.
[3]Research Center for Hepatitis and Immunology, National Center for Global Health and Medicine, Ichikawa, Japan.
*Present affiliation: Department of Virology II, National Institute of Infectious Diseases, Toyama, Tokyo, Japan.

lymphocytes (20,47), leading to the above-mentioned abnormalities. Infection of lymphocytes with HCV has been a matter of debate for a long time. More than one decade ago, several reports described the existence of HCV-RNA in peripheral blood mononucleated cells (PBMCs) (30,40). The detection rate of HCV-RNA in PBMCs was increased if patients were infected with human immunodeficiency virus (HIV) together with HCV (44). This phenomenon indicated that immune-suppressive circumstances and/or HIV antigen might enhance the replication activity of HCV in lymphoid cells (44). Moreover, it was reported that continuous release of HCV by PBMCs was detected in HCV-infected patients, especially in HIV co-infected patients (7). In addition to HCV-HIV co-infected patients, a low level of HCV replication could be detected in peripheral lymphoid cells from HCV mono-infected patients after antiviral treatment (34,45). Moreover, it was reported that HCV persisting at low levels long after therapy-induced resolution of chronic hepatitis C remained infectious (34). This continuous viral presence could present a risk of infection reactivation.

It has been reported that HCV replication was detected in various kinds of lymphoid cells. Many reports describing the existence of HCV in B-lymphocytes and B-cell lymphoma have been published (21,25,51). Among B-lymphocytes, CD27+ memory B-lymphocytes were more resistant to apoptosis than CD27− B-lymphocytes. CD27+ B-lymphocytes were reported as a candidate subset of the HCV reservoir in chronic hepatitis C (CH-C) (38). On the other hand, others claimed that distinguishing RNA association from true HCV replication was problematic, together with multiple artifacts complicated detection and quantitation of the replicative intermediate minus strand RNA (29,31), and also the failure of retroviral (37) and lentiviral (8) pseudoparticles bearing HCV envelope glycoproteins (HCVpp) to infect primary B-cells or B-cell lines. This led to continuous debate about HCV infection into B-lymphocytes, and the riddle remained unsolved.

Using the recent progress in HCV infection systems, we intended to clarify this debate and analyze HCV infection in human lymphocytes and its functional results. Here, albeit in a lower efficiency compared to HCV infection into Huh7 cells, we report that two different strains of recombinant HCV viruses could infect primary human lymphocytes not only by the detection of HCV-RNA positive and negative strands proliferation, but also NS5A protein detection, and the detection of the activity of luciferase reporter encoded by the recombinant HCV-genome. Blocking of HCV entry using anti-CD81 antibody (Ab), and replication by IFN-α or NS3/4A protease inhibitors successfully suppressed HCV infection. We also found that HCV infection into B-lymphocytes led to the initiation of host response including apoptosis resistance.

Materials and Methods

Cells and reagents

Huh7.5.1 cells were kindly provided by Dr. Francis V Chisari (The Scripps Research Institute, La Jolla, CA). Cells were cultured in high-glucose Dulbecco's modified Eagle's medium (DMEM ; Gibco/Invitrogen, Tokyo, Japan) supplemented with 2 mM L-Glutamine, 100 U of penicillin/mL, 100 μg of streptomycin/mL, 1× MEM non-essential amino acid (Gibco/Invitrogen), and 10% fetal bovine serum (FBS).

Human peripheral blood mononuclear cells (PBMCs) were obtained from healthy volunteers by density gradient centrifugation using Ficoll Paque plus (GE-Healthcare, Waukesha, WI). CD19+ blood cells (representative of human primary B-cells) and CD19− cells (non-B-cells) were separated by MACS CD19 Beads (Milteny Biotec, Bergisch Gladbach, Germany). Purity of CD19+ B-cells was >95% after two-cycle separation. The cells were cultured in RPMI1640 (Gibco/Invitrogen) supplemented with 100 U of penicillin/mL, 100 μg of streptomycin/mL, and 10% FBS.

The following reagents were obtained as indicated: anti-CD81 Ab (BD Pharmingen, Franklin Lakes, NJ); PE anti-CD80 Ab, APC anti-CD86 Ab, and PE-labeled anti-CD19 Ab (eBioscience, San Diego, CA); recombinant IFN-α (Peprotech, Oak Park, CA); BILN2601 (Behringer, Willich, Germany); and Viaprobe 7AAD (BD Bioscience) and Annexin-V-Fluos (Roche, Mannheim, Germany).

Virus propagation

pJ6-N2X-JFH1 was kindly provided from Dr. Takaji Wakita (National Institute of Infectious Diseases, Tokyo) (2). pJc1-GLuc2A was gifted from Dr. Brett D. Lindenbach (Yale University, New Haven) (41). *In vitro* RNA transcription, gene transfection into Huh7.5.1 cells, and preparation of J6JFH1 and Jc1/GLuc2A viruses were performed as previously reported (53). Briefly, the HCV cDNA in plasmids were digested by XbaI and transcribed by T7 Megascript Kit (Invitrogen, Carlsbad, CA). RNA transfection into Huh7.5.1 was performed by electroporation using Gene Pulser II (Bio-Rad, Berkeley, CA) at 260 V and 950 Cap. Culture supernatant were collected on days 3, 5, 7, and 9 of postelectroporation, and concentrated with an Amicon Ultra-15 Centrifugal Filter unit (Millipore, Billerica, MA). The titer of HCVcc was checked by the immunofluoresence method using NS5A antibody when Huh7.5.1 was reinfected with these HCVcc.

Virus infection

Primary B-cells and non-B-cells were cultured with the J6JFH1 HCV strain at a multiplicity of infection (MOI) = 1–3 for 3 h, and cells were harvested after four extensive washes in culture medium. On days 1–6, cells were collected, washed with 0.25% trypsin-EDTA/saline, and incubated with 0.25% trypsin-EDTA for 5 min at 37°C. Then, suspended cells were collected as a source of total RNA. In some experiments, B-cells were infected with the Jc1/GLuc2A strain at MOI = 5 for 3 h. Cells were washed five times in 1× phosphate buffered saline (PBS), and cultured until day 6 for determination of viral replication as GLuc activity with BioLux Gaussia luciferase assay kits (41).

RNA purification, RT-PCR, and quantitative PCR

Total RNA was extracted by using Trizol Reagent (Invitrogen) according to the manufacturer's instructions. Using 100–400 ng of total RNA as a template, we performed RT-PCR and real-time RT-PCR as previously described (3,4). Primer sets are shown in Supplementary Table S1 and Table S2 (Supplementary Data are available online at www.liebertpub.com/vim).

Real-time PCR was used for quantification of positive-strand and negative-strand HCV RNA. Total Trizol-extracted

RNA was analyzed by RT-PCR with a modification of the previously described strand-specific rTth RT-PCR method (10,13). RT primers for complementary DNA synthesis of positive and negative strand HCV RNA are shown in Supplementary Table S1. Positive-strand and negative-strand HCV PCR amplifications were performed using Power SYBR Green PCR Master Mix (Applied Biosystems, Warrington, UK) with 200 nM of paired primers (Supplementary Table S1). The PCR conditions were 95°C for 10 min, followed by 40 cycles at 95°C for 15 sec and 60°C for 1 min.

Virus production and releasing assay

Primary human B-cells were infected with J6JFH1 at MOI = 1. Six days postinfection, the supernatant was collected ("releasing samples"), cells were repeatedly frozen and thawed, and the supernatant was collected ("assembly samples"). Viral titers of "releasing samples" and "assembly samples" were determined with Huh7.5.1 cells using J6JFH1 virus (MOI = 0.001 and 0.01) as control. Total RNA was recovered from the cells on days 2, 4, and 6, and determined with HCV-RNA to check reinfectivity.

Indirect immunofluorescence

Indirect immunofluorescence (IF) expression of HCV proteins was detected in the infected cells using rabbit IgG anti-NS5A antibody (C1-1) (3). Goat anti-rabbit Alexa 594 (Invitrogen) was used as secondary Ab. Fluorescence detection was performed on the Zeiss LSM 510 Meta confocal microscope (Zeiss, Jena, Germany) (13).

Luciferase assay

Primary B-cells were infected with Jc1/Gluc2A by using concentrated Medium or Mock Medium (PBS-electropolated Huh7.5.1 medium). Media were collected on days 0, 2, 4, and 6 postinfection, cleared by centrifugation (16,000 *g* for 5 min), and mixed with 0.25 volume of *Renilla* 5 lysis buffer (Promega, Madison, WI) to kill HCV infectivity. GLuc activity was measured on a Berthold Centro LB 960 luminescent plate reader (Berthold Technologies, Bad Wildbad, Germany) with each 20 μL sample injected with 50 μL BilLux Gaussia Luciferase Assay reagent (New England Biolabs, Ipswich, MA), integrated over 1 sec.

Cell survival assay

Apoptosis assay: Primary B cells were infected with J6JFH1 virus. Cells were collected 48 h after infection, stained by 7AAD Cell Viability assay kit and Annexin V, and analyzed by FACS Calibur (BD) (13).

ATP assay

Primary B-cells were infected with J6JFH1 virus or Mock concentrated medium. Cells were resuspended and cultured at Lumine plate (Berthold Technologies) postinfection. ATP activities were determined 72 h later using CellTiter-Glo® Luminescent Cell Viability Assay (Promega) according to the manufacturer's protocol.

miRNA detection

Total RNA was extracted by using Qiazol Reagent (Invitrogen). These RNA was purificated and reverse transcripted to cDNA by using the miScript II RT Kit. Synthesized cDNA was used to determine the expression levels of miR-122 (24). Total miRNA was prepared by using Qiazol and miScript II RT kit (Invitrogen), and miR-122 expression was determined by using miScript SYBR Green PCR Kit and miScript Primer Assay (Invitrogen) according to the manufacturer's protocol. U6 small nuclear RNA was used as an internal control.

Results

J6JFH1 infects and replicates in primary B-cells

To address HCV infectivity into primary B-cells, PBMC were isolated from the blood of healthy volunteers and were sorted into CD19+ cells (primary B-lymphocytes) and CD19− cells (non-B-cells). Their purities were >95%. These cells were then incubated with the J6JFH1 HCV. Total RNA was collected on days 2, 4, and 6. The Huh7.5.1 strain was used as positive control. Both Huh7.5.1 and primary B-cells, but not non-B-cells, showed an increase in intracellular HCV-RNA titer, albeit primary B-cells showed lower efficiency than Huh7.5.1 (Fig. 1A). We adjusted the HCV-RNA values using GAPDH as an internal control (Fig. 1B). To confirm J6JFH1 replication in primary B-cells using IF, we also measured the expression of HCV-NS5A, which is a nonstructural protein produced only by the virus secondary to replication. Although the expression was far lower than Huh7.5.1 cells, we managed to detect the NS5A expression in J6JFH1 infected primary B-cells (Fig. 1C).

We examined what kinds of HCV-entry receptors human primary B-cells expressed in our setting. Human CD81, SRB1, and NPC1L1 were expressed, but not the tight junction proteins claudin1 and occludin in mRNA levels (Supplementary Fig. S1). We could not detect miR122 in primary B-cells (Supplementary Fig. S2), expression of which makes the cells permissive to HCV (24). Human CD81 is a primary entry receptor for HCV in hepatocytes (42). Blocking human CD81 by its specific Ab resulted in blockage of HCV infection into primary B-cells, as shown by the suppression of HCV-RNA titer (Fig. 2), suggesting that HCVcc particles enter B-cells also using CD81 receptor. HCV-RNA titer was not suppressed by non-specific Ab (data not shown).

We then examined the effect of the different drugs used to suppress HCV replication (recombinant human IFN, and HCV protease inhibitor, BILN2601). Inhibition of HCV-RNA replication was observed when B-cells were treated with rhIFN-α or BILN2601 (Fig. 2) after infection. BILN2601 showed efficient inhibitory effect on replication of HCV RNA in Huh7.5.1 cells (Supplementary Fig. S3). As control studies, we confirmed that the production of HCV RNA was reduced in Huh7.5.1 cells by CD81 Ab, IFN-α, or BLIN2601 (Supplementary Fig. S4). In both Huh 7.5.1 and B-cells, BLIN2601 most effectively block HCV replication. These data reinforce that HCV is actually replicating in primary B-cells, and that activation of innate immunity by IFN treatment or blocking the NS3/4A protease function is a critical factor in blocking HCV replication in primary B-cells. These data suggest that our system can be used for screening the function of different inhibitors on HCV replication in B-cells.

HCV negative-strand RNA detected in human B-cells

To confirm HCV replication in primary B-cells further, we tested for an increase of negative-strand HCV-RNA after

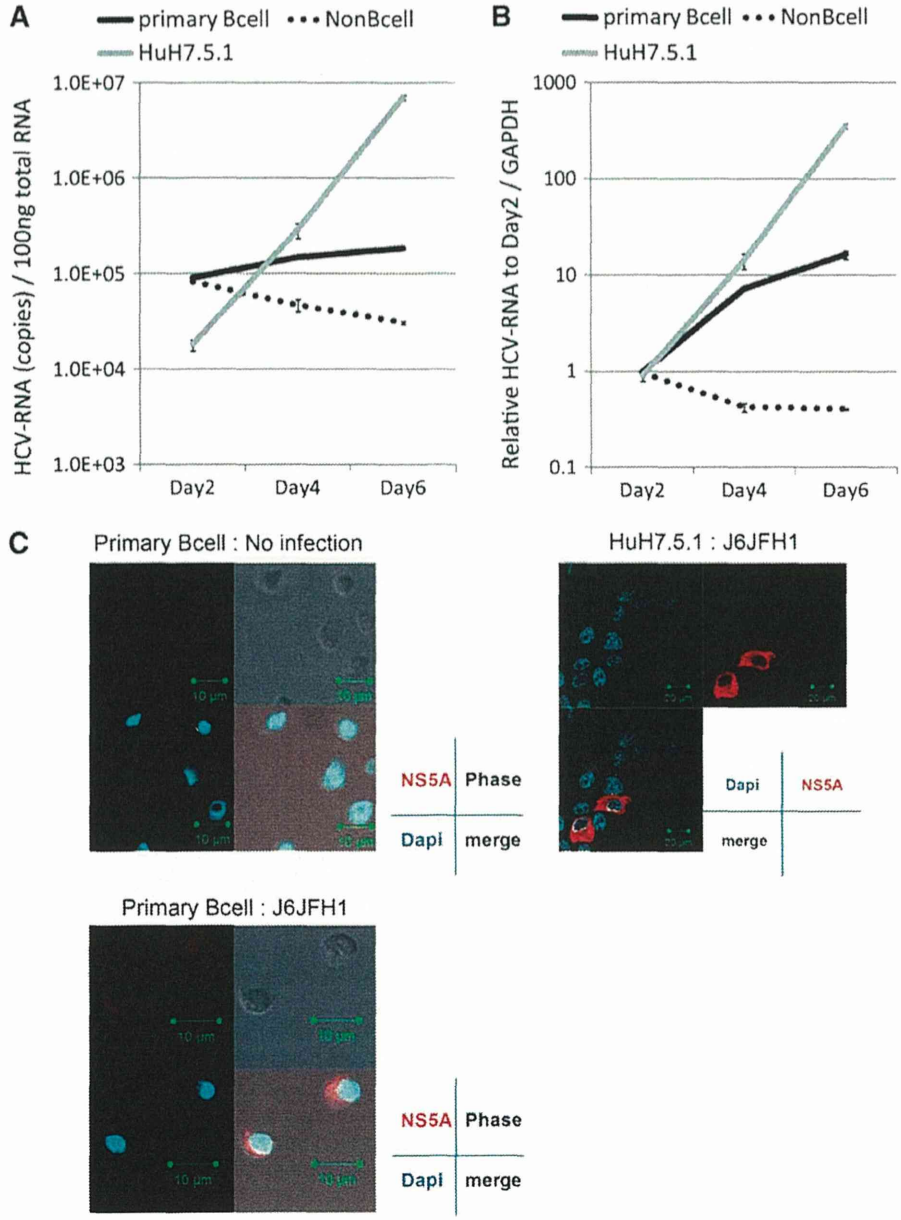

FIG. 1. J6JFH1 infects human peripheral blood B-cells. Human B-cells (CD19+ cells) and non-B-cells (CD19− cells) were separated by MACS as described in Materials and Methods. Primary B-cells, non-B-cells, and Huh7.5.1 cells were infected with J6JFH1 at $MOI = 1$ for 3 h. After infection, cells were washed twice with culture medium and continued culture. On days 2, 4, and 6, total RNA was collected and HCV-derived RNA was determined by reverse transcription polymerase chain reaction (RT-PCR). GAPDH was used as internal control. **(A)** HCV-RNA not adjusted by GAPDH. **(B)** HCV-RNA adjusted by GAPDH. **(C)** Immunofluorescence analysis of J6JFH1-infected human B-cells and Huh7.5.1 cells. Six days postinfection. Red, NS5A; blue: Dapi; phase: phase-shift microscope.

infection, since the negative-strand RNA is not yielded if HCV particles or RNA just adhere to the cell surface of human primary B-cells without internalization (9,14,19,35, 42,43). We measured the synthesis of plus-strand and minus-strand HCV-RNA separately using strand-specific RT primers and rTth polymerase as previously described (4). The titer increase of minus-strand HCV-RNA indicates HCV-RNA replication. As shown in Figure 3, both minus- and plus-strand HCV-RNA increased time dependently in primary B-cells, and both types of RNA concomitantly decreased in non-B-cells (Fig. 3A and B). Plus- and minus-strand RNA were exponentially increased in Huh7.5.1 cells infected with J6JFH1 (Fig. 3C). These results indicated that primary human B-cells supported J6JFH1 infection and replication, although viral replication levels in B-cells were modest compared with those in Huh7.5.1 cells. These results